Electronic Supplementary Material (ESI) for Dalton Transactions.

Supporting Information

Enhanced kinetic stability of $[Pd_2L_4]^{4+}$ cages through ligand substitution

Dan Preston,[a] Samantha M. McNeill,[b] James E. M. Lewis,[a] Gregory. I. Giles,[b] and James D. Crowley[a]*

[a] Department of Chemistry, University of Otago, PO Box 56, Dunedin, New Zealand.
[b] Department of Pharmacology and Toxicology, University of Otago, PO Box 56, Dunedin, New Zealand.

***jcrowley@chemistry.otago.ac.nz**

Contents

1 Experimental

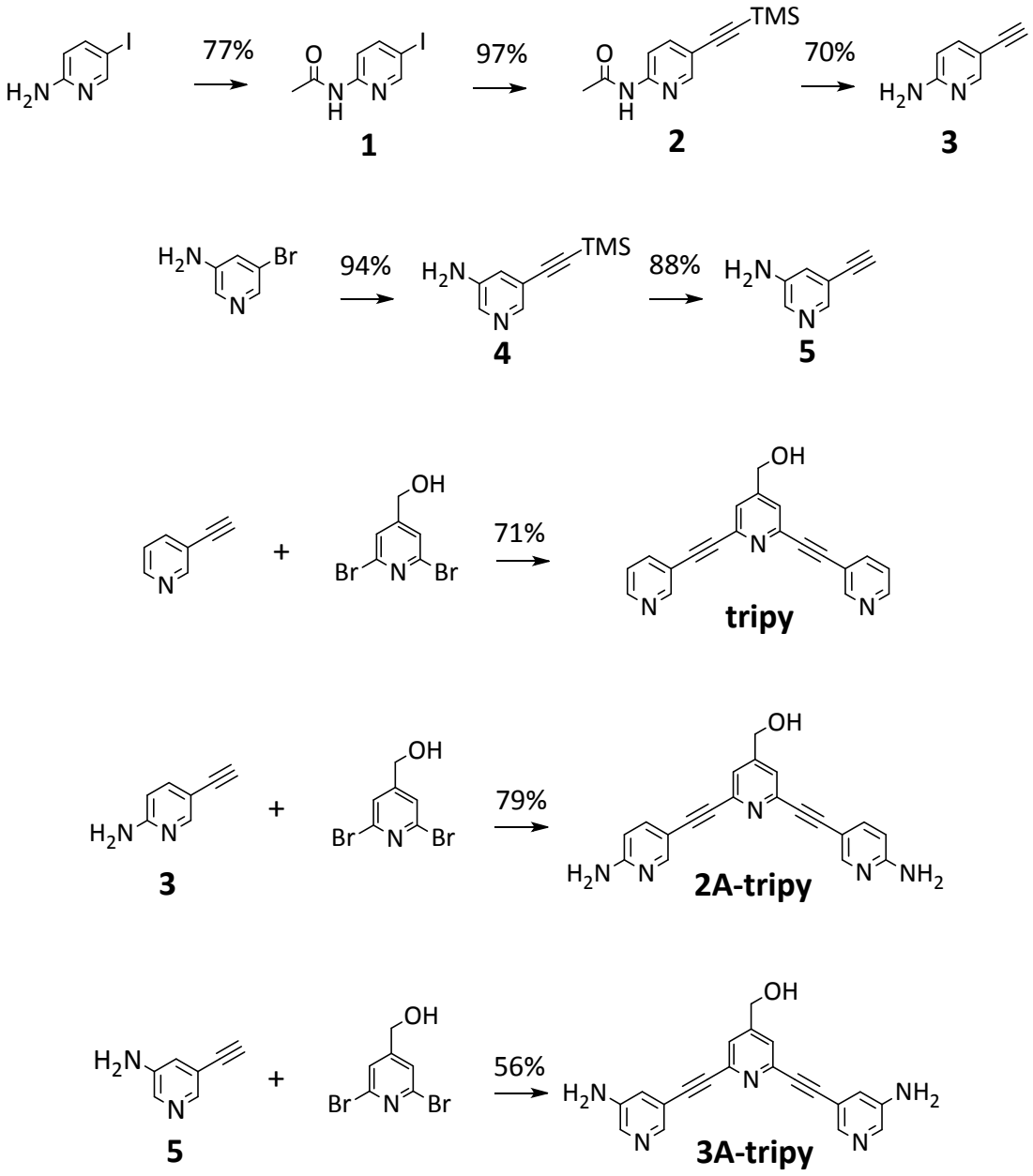

Scheme S1. Synthesis of the tripyridyl ligands, **tripy**, **2A-tripy** and **3A-tripy**.

1.1 NMR spectral data, 1

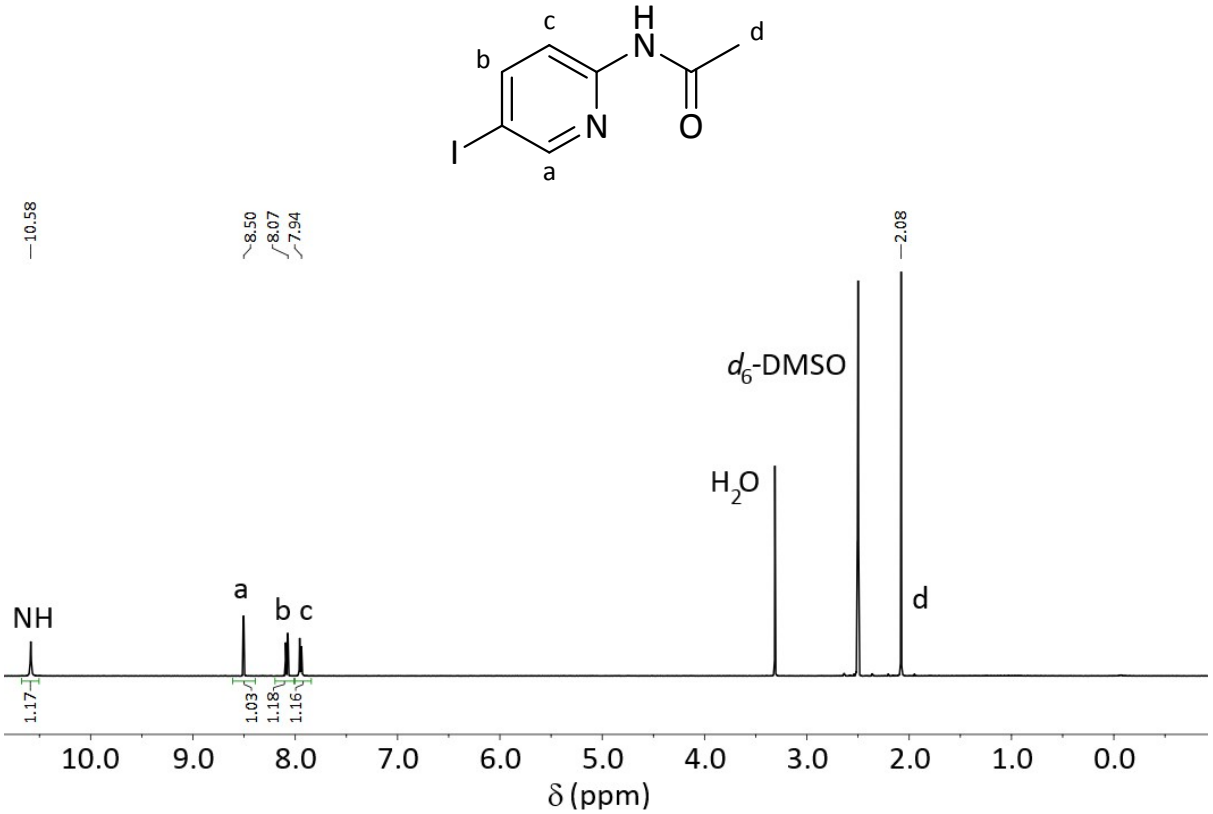

Figure S1.1 ^{1}H NMR spectrum (400 MHz, d_6-DMSO, 298 K) of **1**.

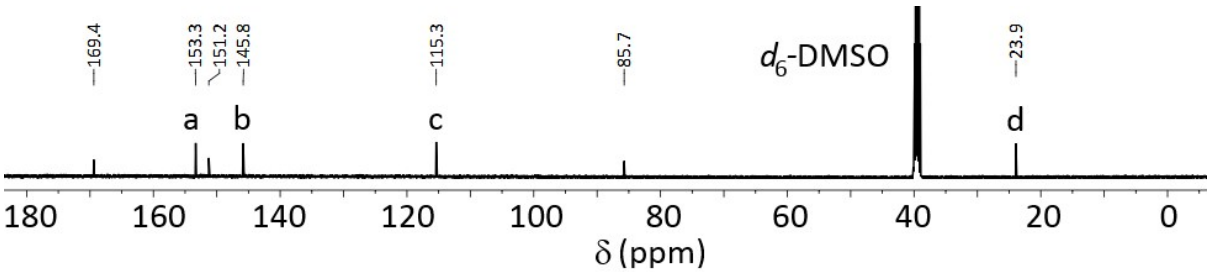

Figure S1.2 ^{13}C NMR spectrum (100 MHz, d_6-DMSO, 298 K) of **1**.

1.2 NMR spectral data, 2

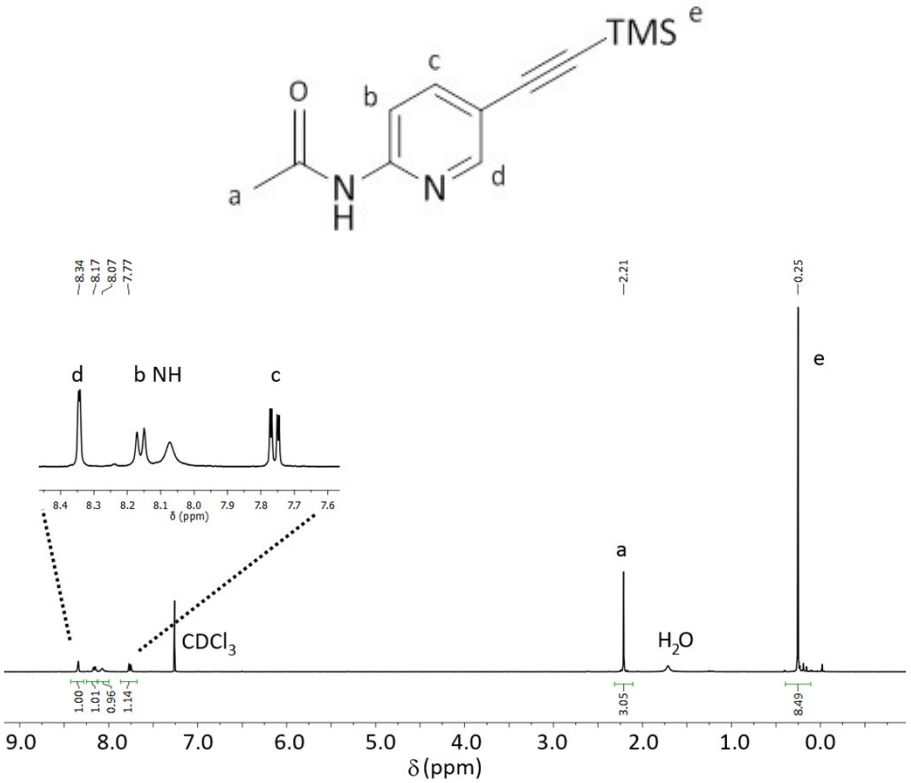

Figure S1.3 ^{1}H NMR spectrum (500 MHz, $CDCl_3$, 298 K) of **2**.

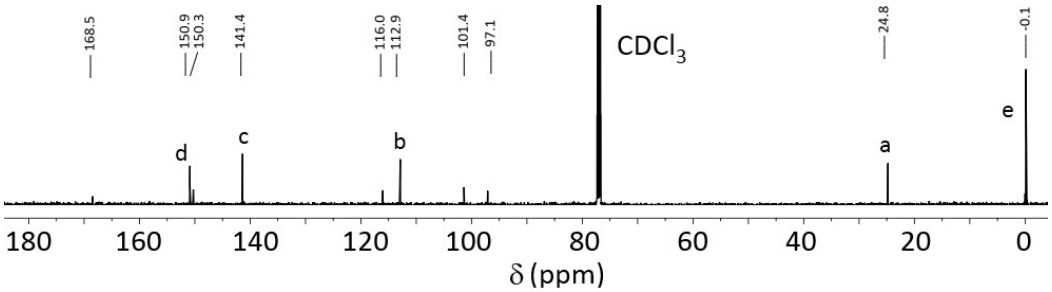

Figure S1.4 ^{13}C NMR spectrum (125 MHz, $CDCl_3$, 298 K) of **2**.

1.3 NMR spectral data, 3

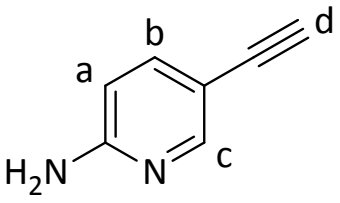

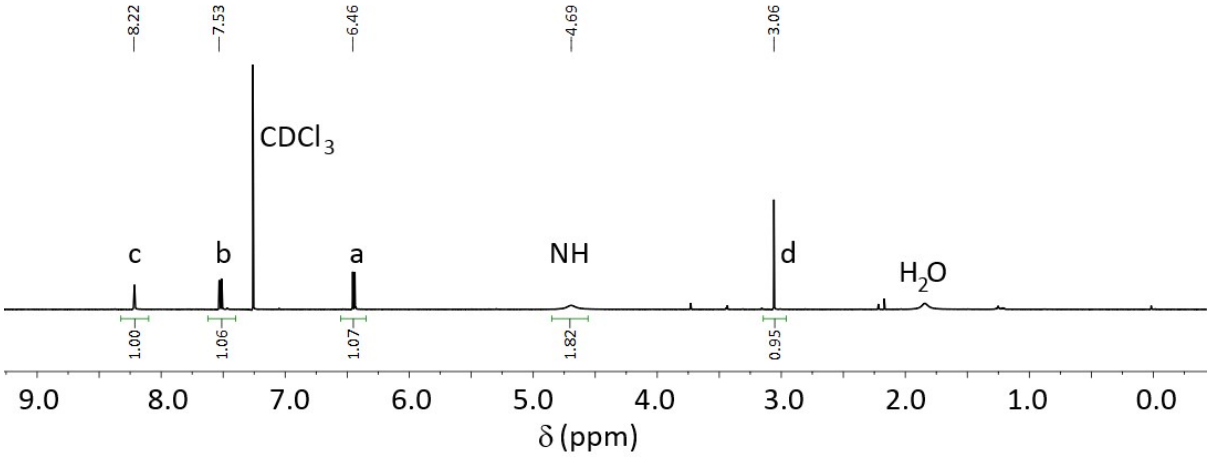

Figure S1.5 ^{1}H NMR spectrum (500 MHz, $CDCl_3$, 298 K) of **3**.

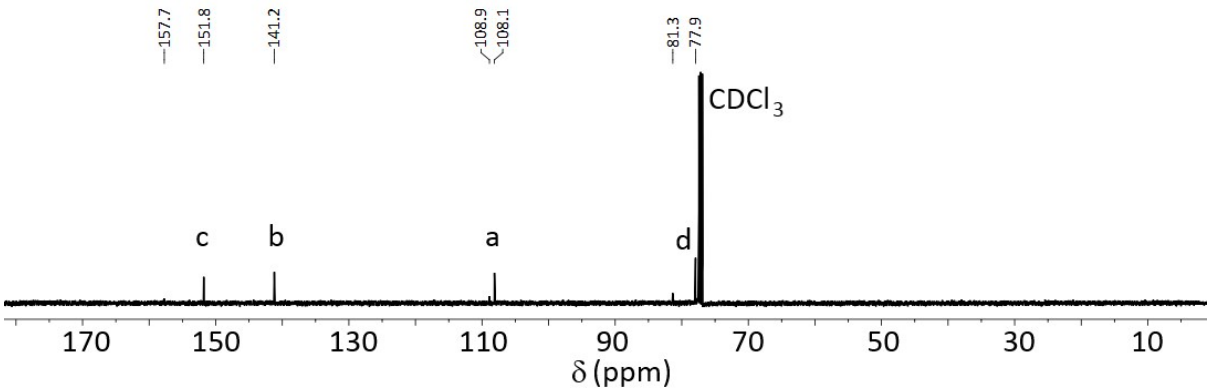

Figure S1.6 ^{13}C NMR spectrum (125 MHz, $CDCl_3$, 298 K) of **3**.

1.4 NMR spectral data, 4

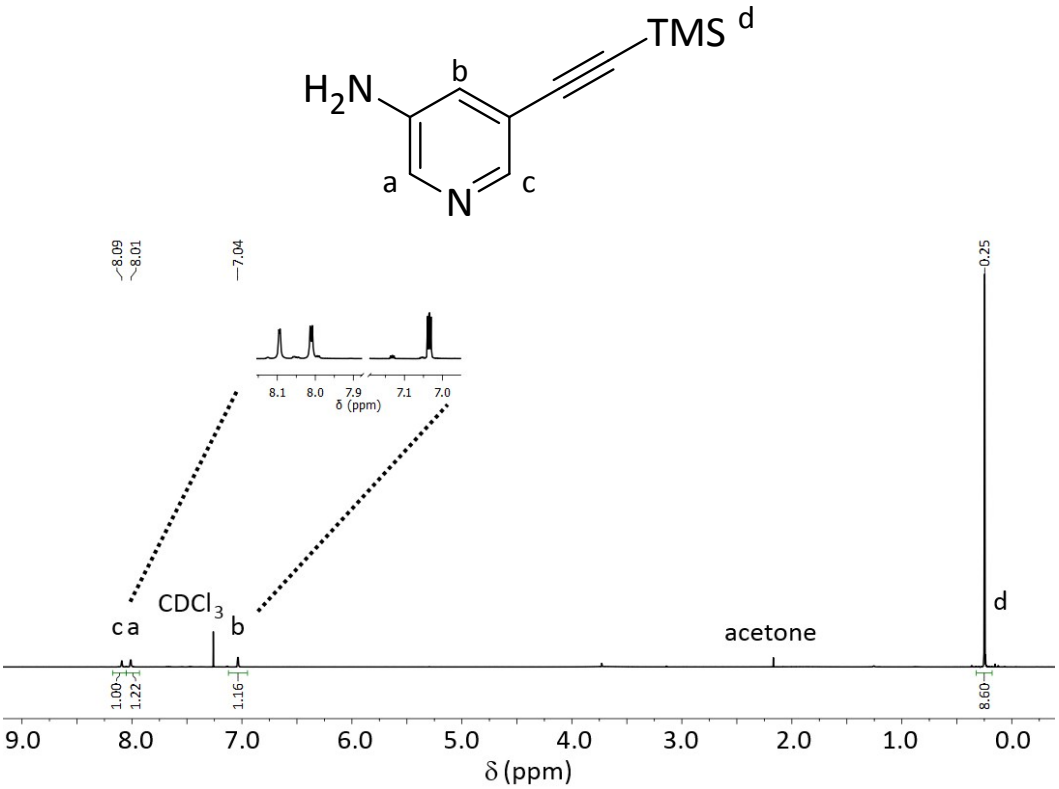

Figure S1.7 ^{1}H NMR spectrum (500 MHz, $CDCl_3$, 298 K) of **4**.

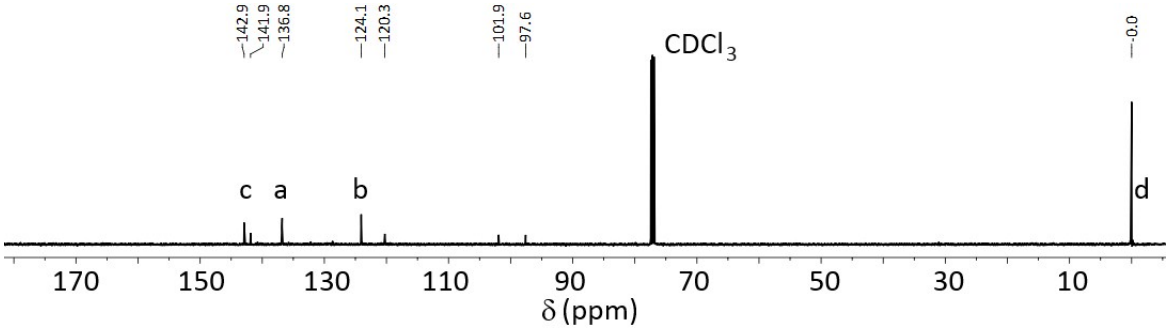

Figure S1.8 ^{13}C NMR spectrum (125 MHz, $CDCl_3$, 298 K) of **4**.

1.5 NMR spectral data, 5

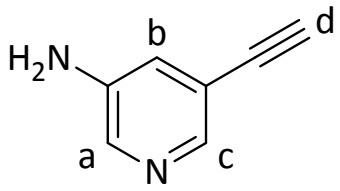

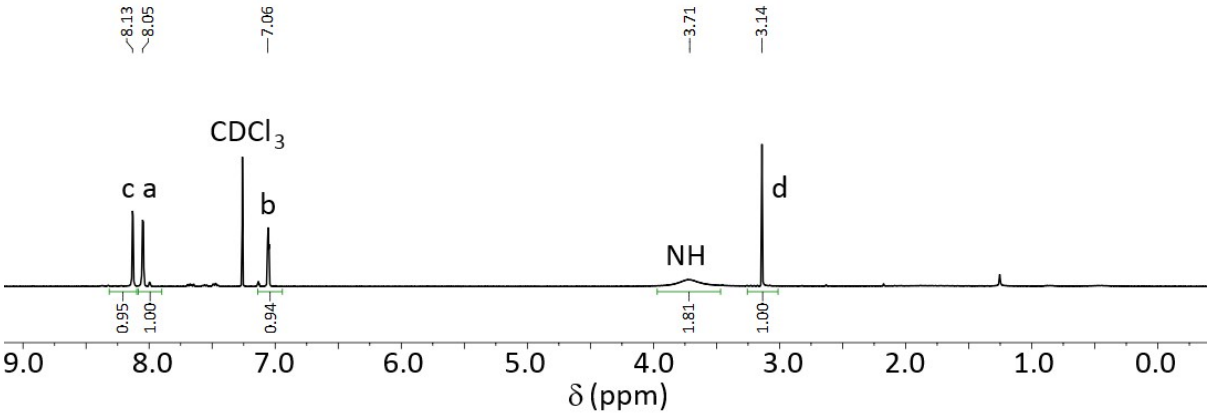

Figure S1.9 ^{1}H NMR spectrum (500 MHz, $CDCl_3$, 298 K) of **5**.

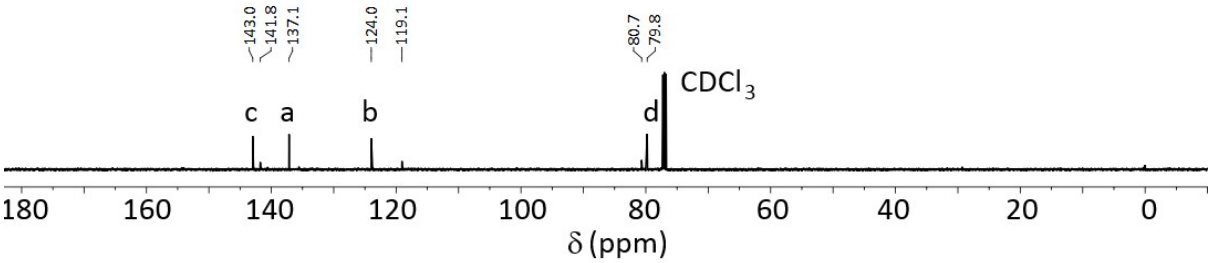

Figure S1.10 ^{13}C NMR spectrum (125 MHz, $CDCl_3$, 298 K) of **5**.

1.6 NMR spectral data, tripy

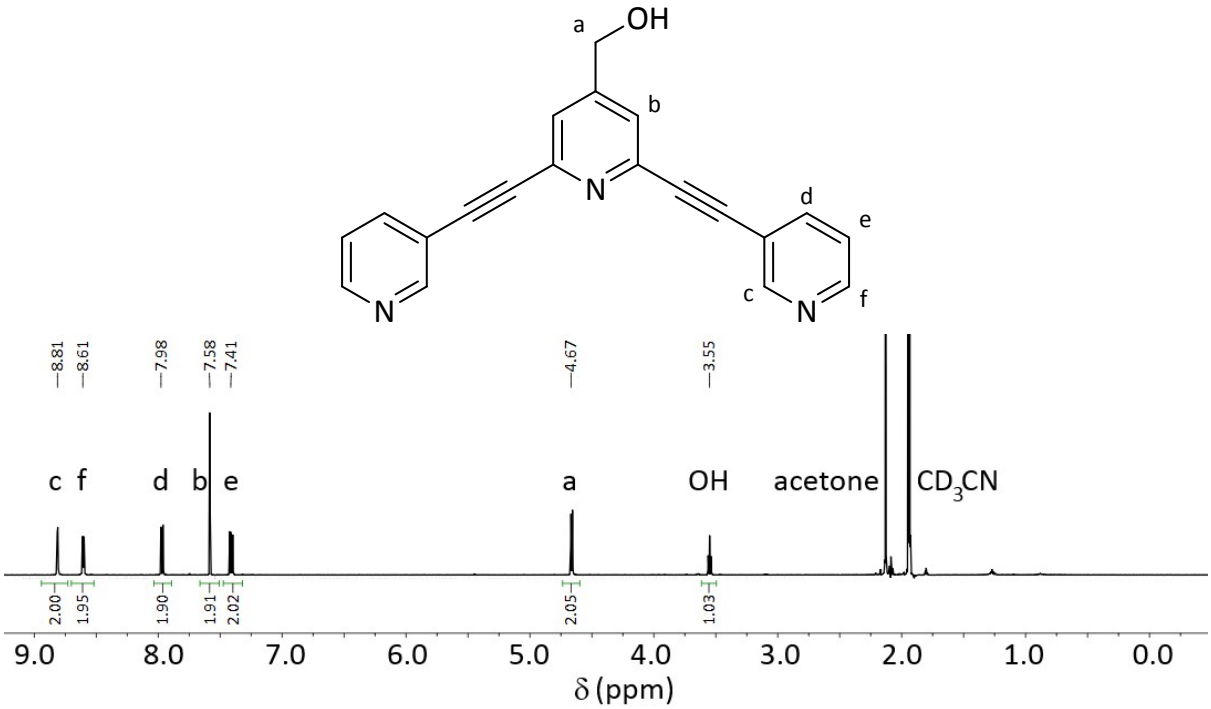

Figure S1.11 ^{1}H NMR spectrum (500 MHz, CD_3CN, 298 K) of **tripy**.

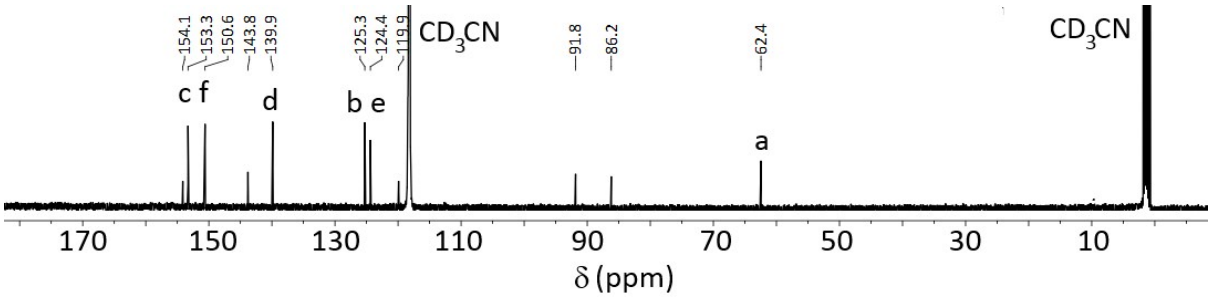

Figure S1.12 ^{13}C NMR spectrum (125 MHz, CD_3CN, 298 K) of **tripy**.

1.7 NMR spectral data, 2A-tripy

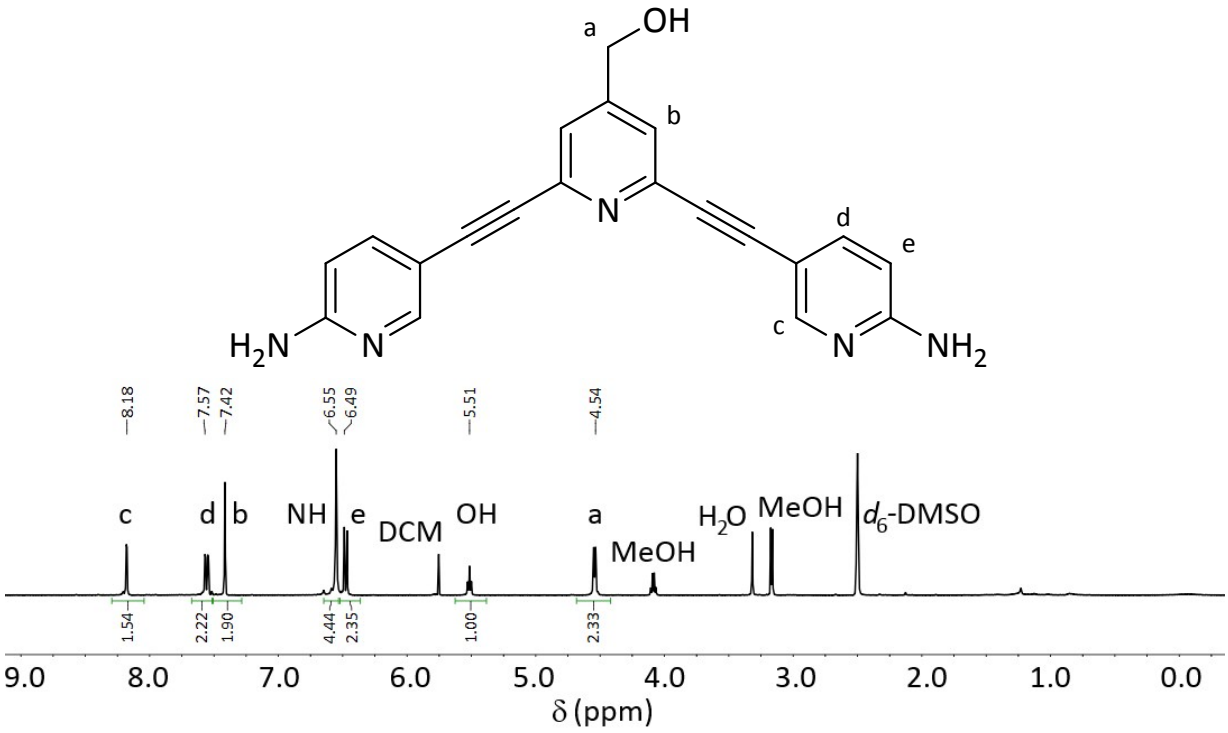

Figure S1.13 ^{1}H NMR spectrum (500 MHz, d_6-DMSO, 298 K) of **2A-tripy**.

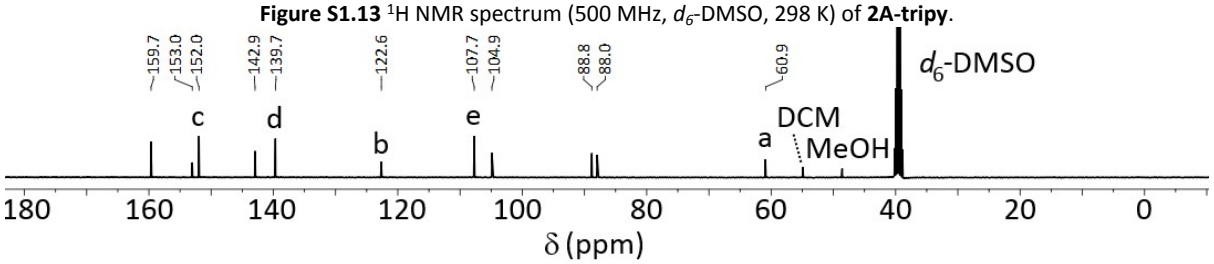

Figure S1.14 ^{13}C NMR spectrum (100 MHz, d_6-DMSO, 298 K) of **2A-tripy**.

1.8 NMR spectral data, 3A-tripy

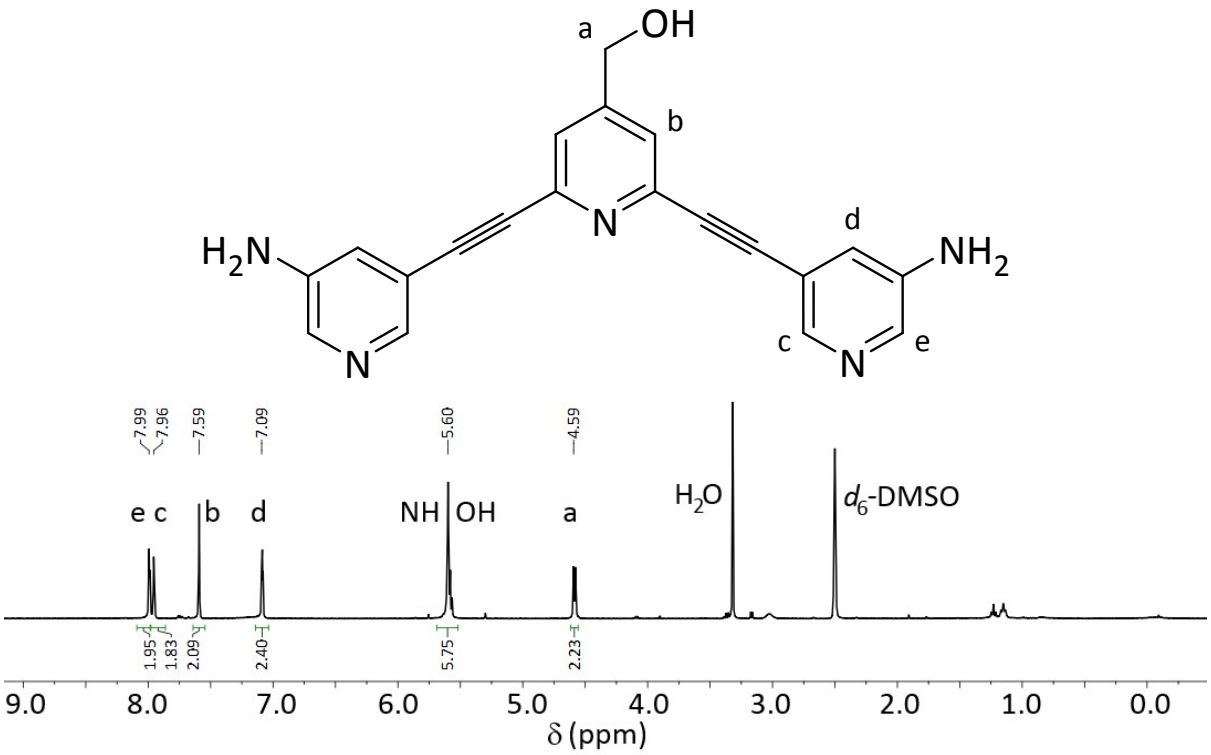

Figure S1.15 ^{1}H NMR spectrum (500 MHz, CD_3CN, 298 K) of **3A-tripy**.

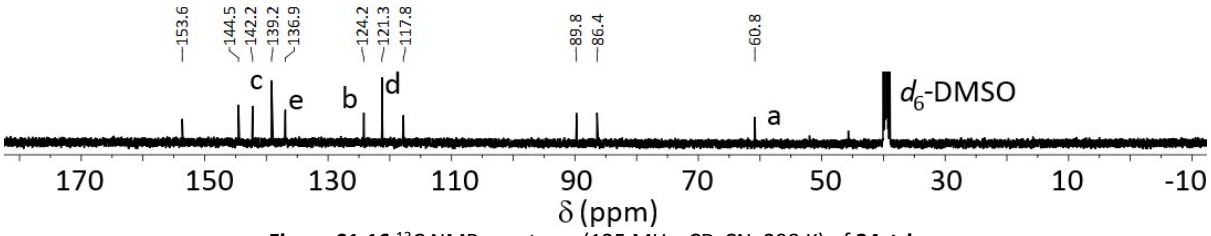

Figure S1.16 ^{13}C NMR spectrum (125 MHz, CD_3CN, 298 K) of **3A-tripy**.

1.9 NMR spectral data, $[Pd_2(tripy)_4](BF_4)_4$

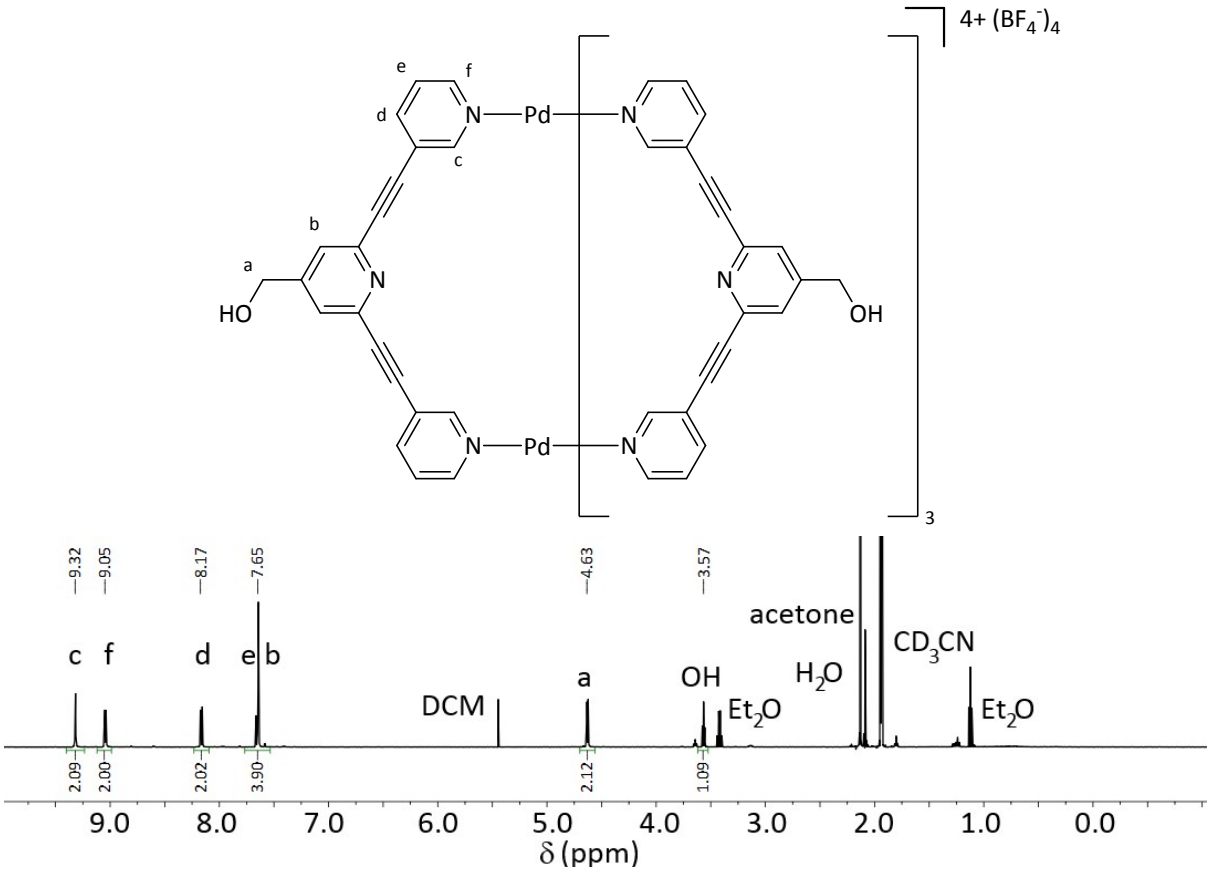

Figure S1.17 ^{1}H NMR spectrum (500 MHz, CD_3CN, 298 K) of $[Pd_2(\mathbf{tripy})_4](BF_4)_4$.

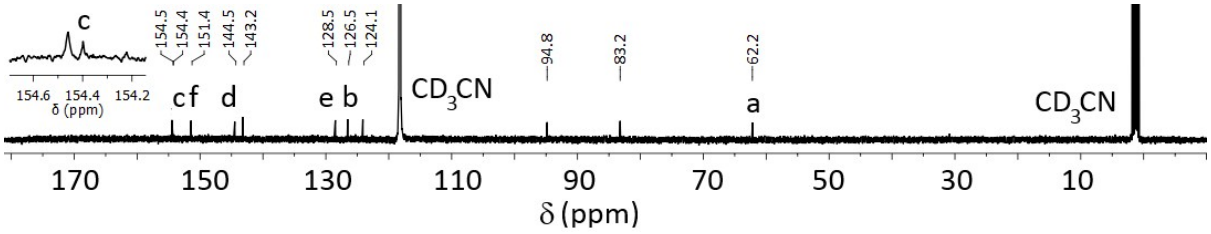

Figure S1.18 ^{13}C NMR spectrum (125 MHz, CD_3CN, 298 K) of $[Pd_2(\mathbf{tripy})_4](BF_4)_4$.

1.10 NMR spectral data, $[Pd_2(2A\text{-}tripy)_4](BF_4)_4$

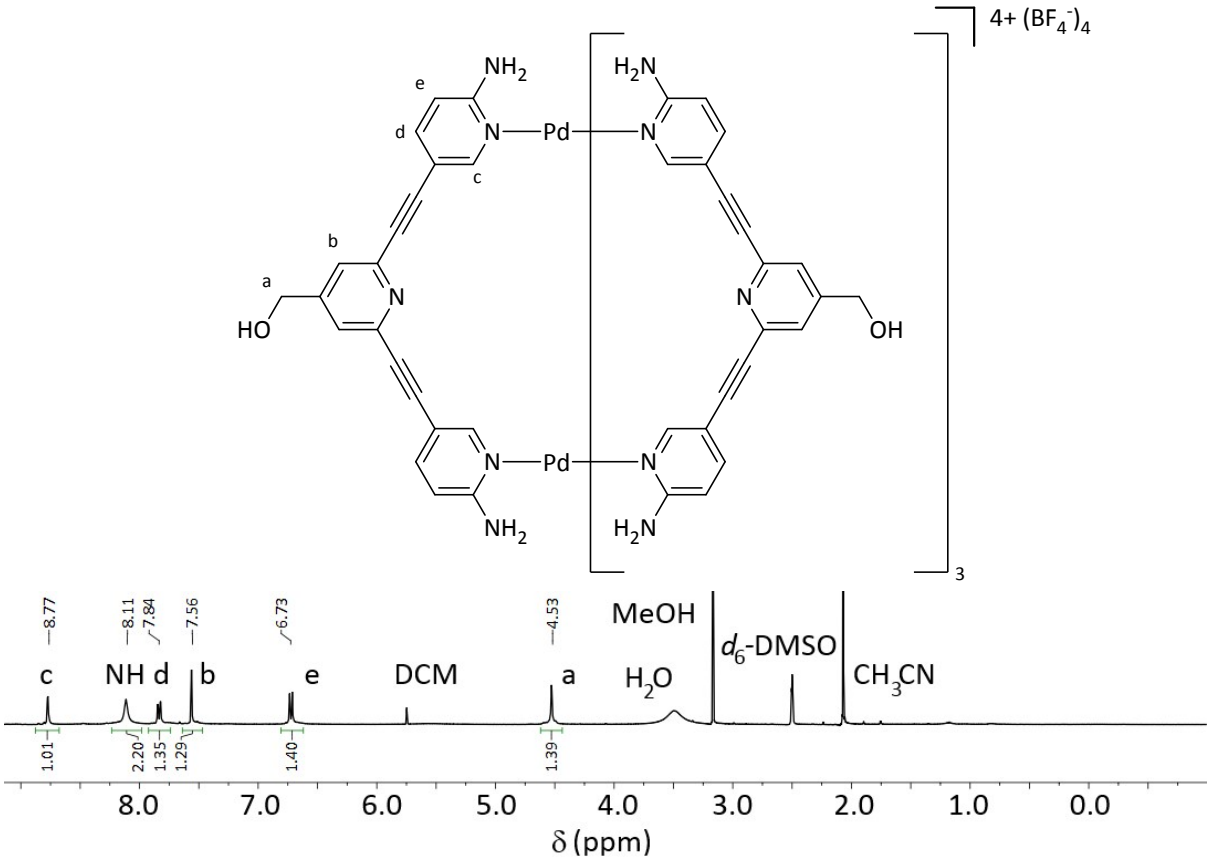

Figure S1.19 ^{1}H NMR spectrum (500 MHz, CD_3CN, 298 K) of $[Pd_2(\mathbf{2A\text{-}tripy})_4](BF_4)_4$.

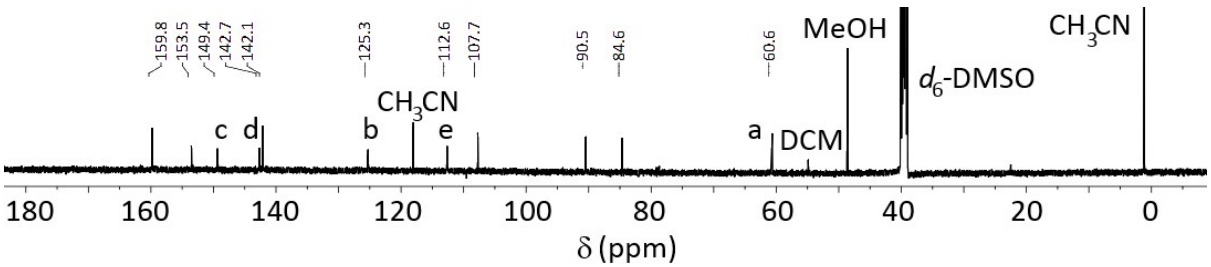

Figure S1.20 ^{13}C NMR spectrum (125 MHz, CD_3CN, 298 K) of $[Pd_2(\mathbf{2A\text{-}tripy})_4](BF_4)_4$.

1.11 NMR spectral data, $[Pd_2(3A\text{-}tripy)_4](BF_4)_4$

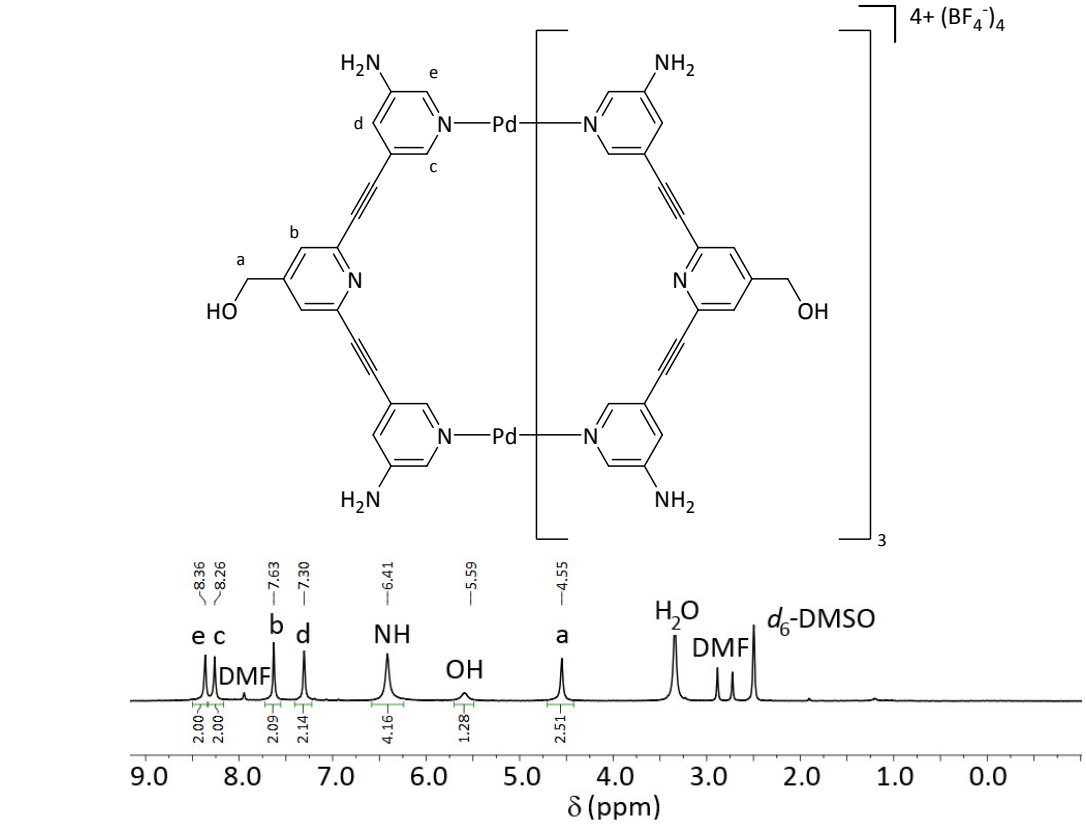

Figure S1.21 ^{1}H NMR spectrum (500 MHz, d_6-DMSO, 298 K) of $[Pd_2(\mathbf{3A\text{-}tripy})_4](BF_4)_4$.

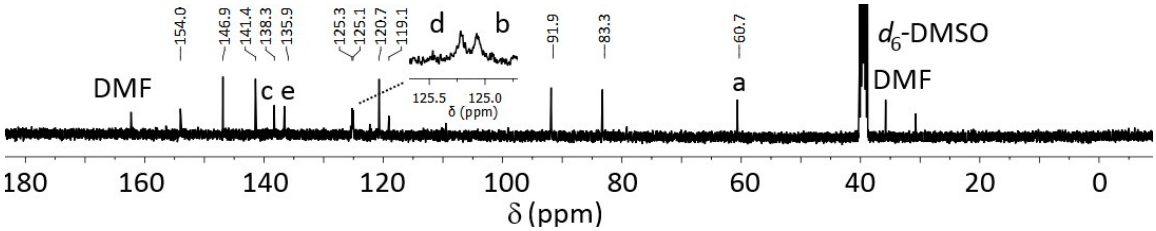

Figure S1.22 ^{13}C NMR spectrum (125 MHz, d_6-DMSO, 298 K) of $[Pd_2(\mathbf{3A\text{-}tripy})_4](BF_4)_4$.

1.12 Synthesis of *trans*-dibromo(1,3-diisopropylbenzimidazolin-2-ylidene)(2-aminopyridine)palladium(II)

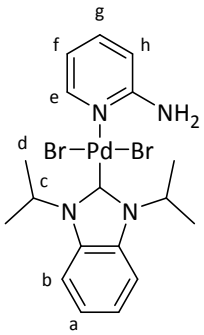

A solution of 2-aminopyridine (3.95 mg, 0.042 mmol) and dibromobis(benzimidazolin-2-ylidene)dipalladium(II) (20 mg, 0.021 mmol) in $CDCl_3$ (0.75 mL) was sonicated for 30 seconds. Vapour diffusion of diethyl ether into this solution gave a yellow semi-crystalline precipitate (15.1 mg, 0.026 mmol, 64%). ^{1}H NMR (400 MHz, $CDCl_3$, 298 K) δ: 8.47 (1H, d, J = 7.0 Hz, H_e), 7.60 (2H, dd, J = 8.2 Hz, 3.2 Hz, H_b), 7.44 (1H, t, J = 8.2 Hz, H_g), 7.24 (2H, dd, J = 8.2 Hz, 3.2 Hz, H_a), 6.69 (1H, t, J = 5.9 Hz, H_f), 6.57 (1H, d, J = 8.3 Hz, H_h), 6.35 (2H, sept, J = 7.0 Hz, H_c), 5.56 (2H, br, H_{NH}), 1.83 (12 H, d, J = 7.0 Hz, H_d). ^{13}C NMR (100 MHz, $CDCl_3$, 298 K) δ: 161.2 ($C_{carbene}$), 158.5, 150.0 (C_e), 138.8 (C_g), 133.6, 122.4 (C_a), 114.4 (C_f), 112.8 (C_b), 115.5 (C_h), 54.8 (C_c), 20.9 (C_d). HR ES-MS (CH_3OH) m/z = 483.0167 $[M - Br]^+$ (calc. for $C_{18}H_{24}BrN_4Pd$, 483.0215), 584.9237 $[M + Na]^+$ (calc. for $C_{18}H_{24}Br_2N_4NaPd$, 584.9284). IR: ν (cm^{-1}) 3419, 3326, 2977, 1623, 1410, 1364, 1306, 1141, 744. Anal. calcd. for $C_{18}H_{24}Br_2N_4Pd$: C, 38.42; H, 4.30; N, 9.96. Found: C, 38.69; H, 4.32; N, 9.94%.

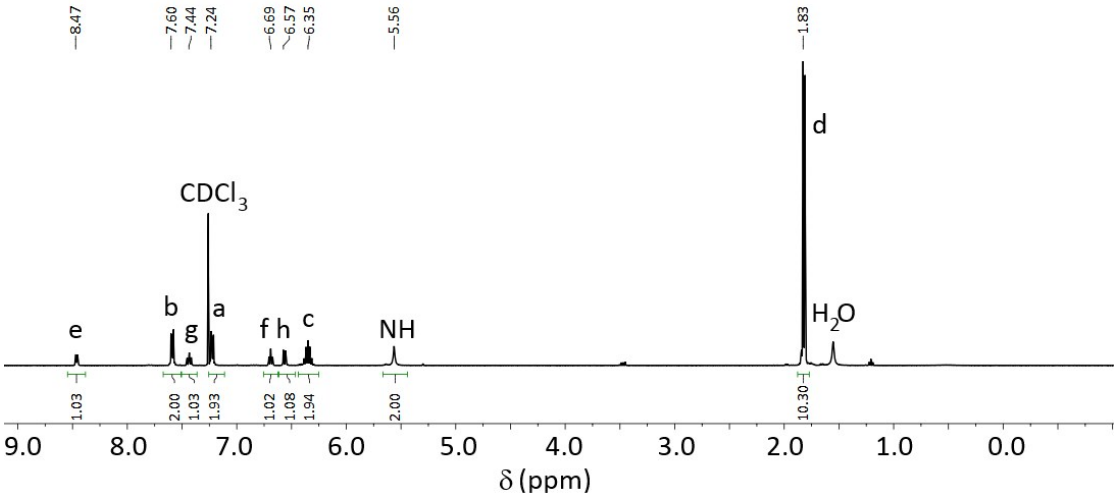

Figure S1.23 ^{1}H NMR spectrum (400 MHz, $CDCl_3$, 298 K) of *trans*-[Pd(NHC)(**2A-py**)](Br_2).

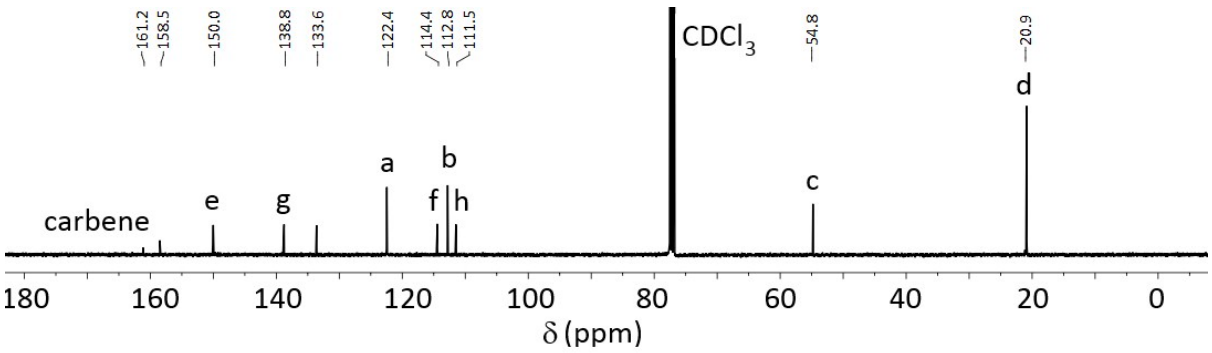

Figure S1.24 ^{13}C NMR spectrum (100 MHz, $CDCl_3$, 298 K) of *trans*-[Pd(NHC)(**2A-py**)](Br_2).

1.13 Synthesis of *trans*-dibromo(1,3-diisopropylbenzimidazolin-2-ylidene)(3-aminopyridine)palladium(II)

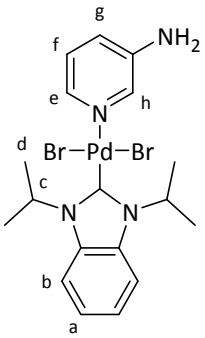

A solution of 3-aminopyridine (10.4 mg, 0.042 mmol) and dibromobis(benzimidazolin-2-ylidene)dipalladium(II) (20 mg, 0.021 mmol) in $CDCl_3$ (0.75 mL) was sonicated for 30 seconds. Vapour diffusion of diethyl ether into this solution gave a yellow precipitate (16.0 mg, 0.028 mmol, 68%). ^{1}H NMR (400 MHz, $CDCl_3$, 298 K) δ: 8.52 (1H, d, J = 2.4 Hz, H_h), 8.46 (1H, d, J = 5.1 Hz, H_e), 7.58 (2H, dd, J = 6.2 Hz 3.2 Hz, H_b), 7.21 (2H, dd, J = 6.1 Hz, J = 3.1 Hz, H_a), 7.07 (1H, dd, J = 8.6 Hz, 5.7 Hz, H_f), 7.00 (2H, d, J = 8.3 Hz, H_g), 6.33 (2H, sept, J = 7.0 Hz, H_c), 3.84 (2H, br, H_{NH}), 1.80 (12H, d, J = 6.9 Hz, H_d). ^{13}C NMR (100 MHz, $CDCl_3$, 298 K) δ: 159.9 ($C_{carbene}$), 143.3, 142.7 (C_e), 139.9 (C_h), 133.6, 124.6 (C_f), 123.1 (C_g), 122.3 (C_a), 112.7 (C_b), 54.6 (C_c), 20.7 (C_d). HR ES-MS (CH_3OH) m/z = 401.0923 [M – HBr – Br]$^+$ (calc. for $C_{18}H_{23}N_4Pd$, 401.0952). IR: ν (cm^{-1}) 3419, 3326, 2977, 1623, 1481, 1410, 1364, 1307, 1141, 1089, 744. Anal. calcd. for $C_{18}H_{24}Br_2N_4Pd$: C, 38.42; H, 4.30; N, 9.96%; found: C, 38.42; H, 4.37; N, 9.91%.

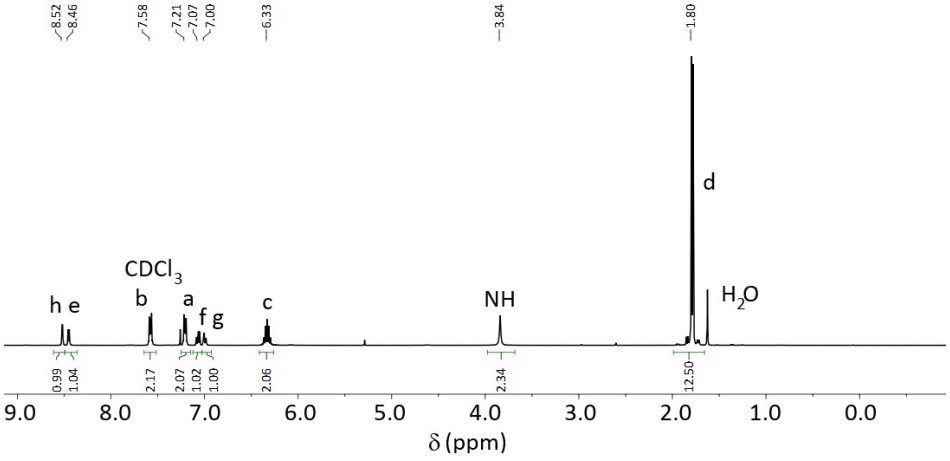

Figure S1.25 ^{1}H NMR spectrum (400 MHz, $CDCl_3$, 298 K) of *trans*-[Pd(NHC)(**3A-py**)](Br_2).

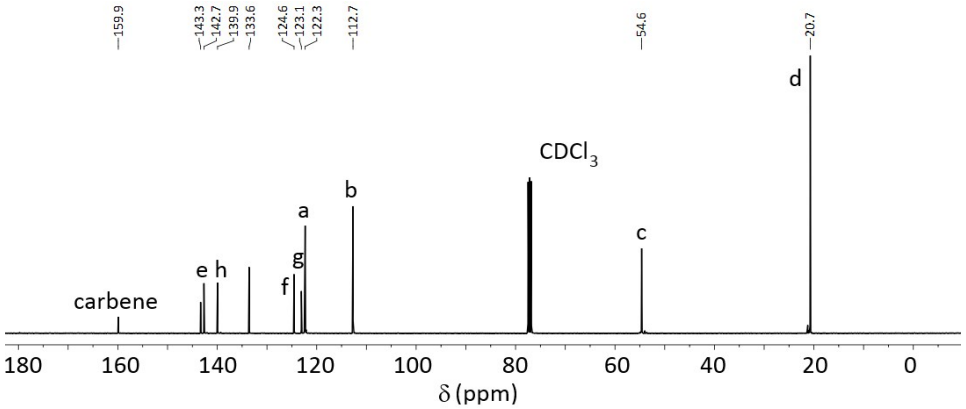

Figure S1.26 ^{13}C NMR spectrum (100 MHz, $CDCl_3$, 298 K) of *trans*-[Pd(NHC)(**3A-py**)](Br_2).

1.14 Synthesis of $[Pd_2(tripy)_4](NO_3)_4$

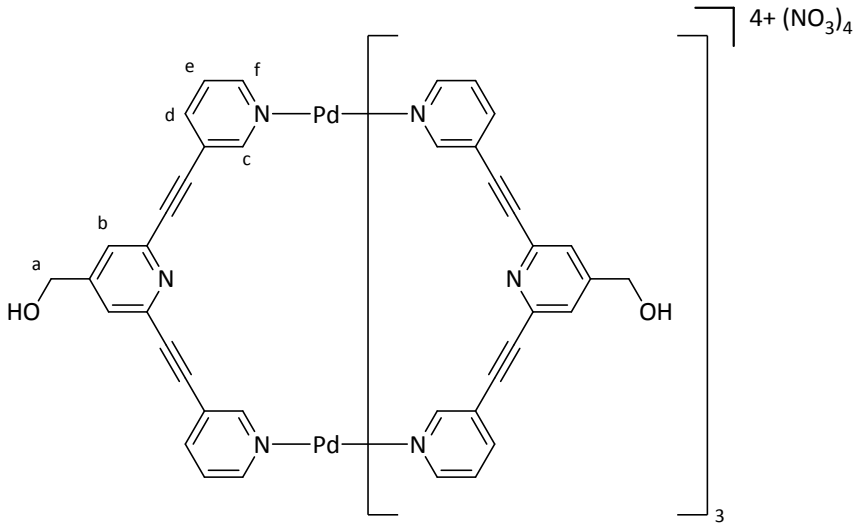

A solution of **tripy** (40 mg, 0.13 mmol) and $Pd(NO_3)_2{\cdot}2H_2O$ (17.9 mg, 0.07 mmol) in d_6-DMSO (1 mL) was sonicated for five minutes. Addition of ethyl acetate (20 mL) resulted in precipitation of the product. The precipitate was collected by filtration, and washed with ethyl acetate (15 mL) and diethyl ether (15 mL) to give a tan solid (40 mg, 0.023 mmol, 73%). ^{1}H NMR (500 MHz, d_6-DMSO, 298 K) δ: 9.88 (8H, s, H_c), 9.41 (1H, d, J = 5.8 Hz, H_f), 8.34 (8H, dd, J = 8.0 Hz, 1.2 Hz, H_d), 7.85 (8H, t, J = 6.8 Hz, H_e), 7.69 (8H, s, H_b), 4.58 (8H, s, H_a). ^{13}C NMR (125 MHz, d_6-DMSO, 298 K) δ: 153.8 (C_c), 153.6, 151.0 (C_f), 143.3 (C_d), 141.7, 127.3 (C_e), 125.6 (C_b), 121.7, 93.6, 83.0, 60.7 (C_a). ESI-MS (DMSO/CH_3CN) m/z = 364.60 $[M - 4(NO_3)]^{4+}$ (calc. for $C_{80}H_{52}N_{12}O_4Pd_2$, 364.60), 364.0759 $[Pd(\mathbf{tripy})_2]^{2+}$ (calc. for $C_{40}H_{26}N_6O_2Pd$, 364.0759). IR: ν (cm^{-1}) 3061, 1592, 1546, 1340. Anal. calcd. for $C_{80}H_{52}N_{16}O_{16}Pd_2{\cdot}3H_2O$: C, 54.59; H, 3.32; N, 12.73%. Found: C, 54.37; H, 3.37; N, 12.50%.

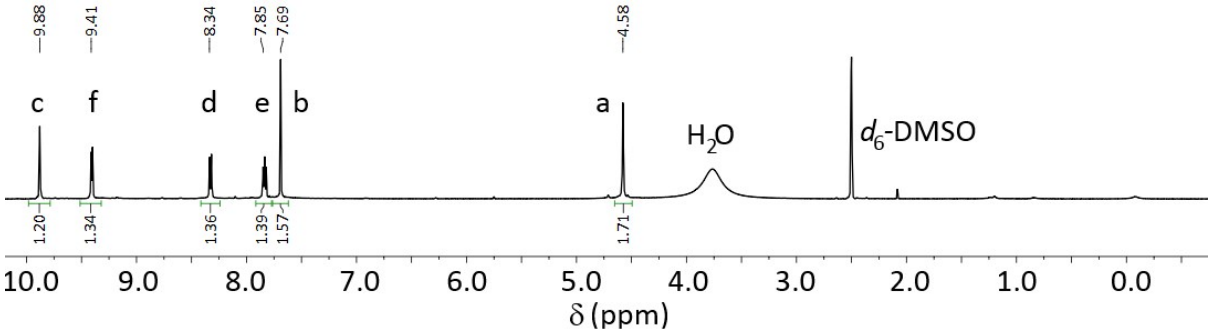

Figure S1.27 ^{1}H NMR spectrum (500 MHz, CD_3CN, 298 K) of $[Pd_2(\mathbf{tripy})_4](NO_3)_4$.

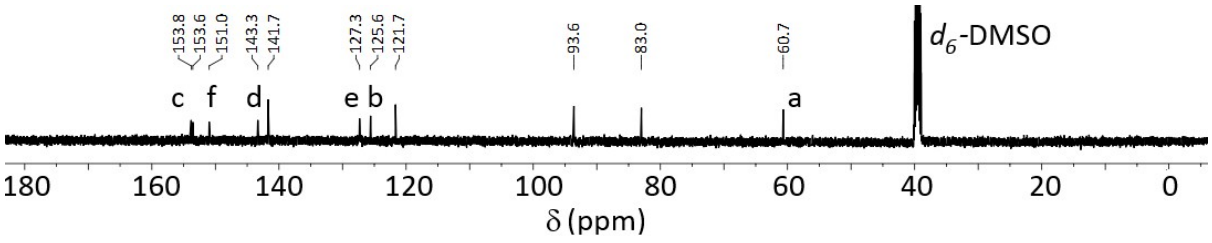

Figure S1.28 ^{13}C NMR spectrum (125 MHz, CD_3CN, 298 K) of $[Pd_2(\mathbf{tripy})_4](NO_3)_4$.

2 Representative mass spectra

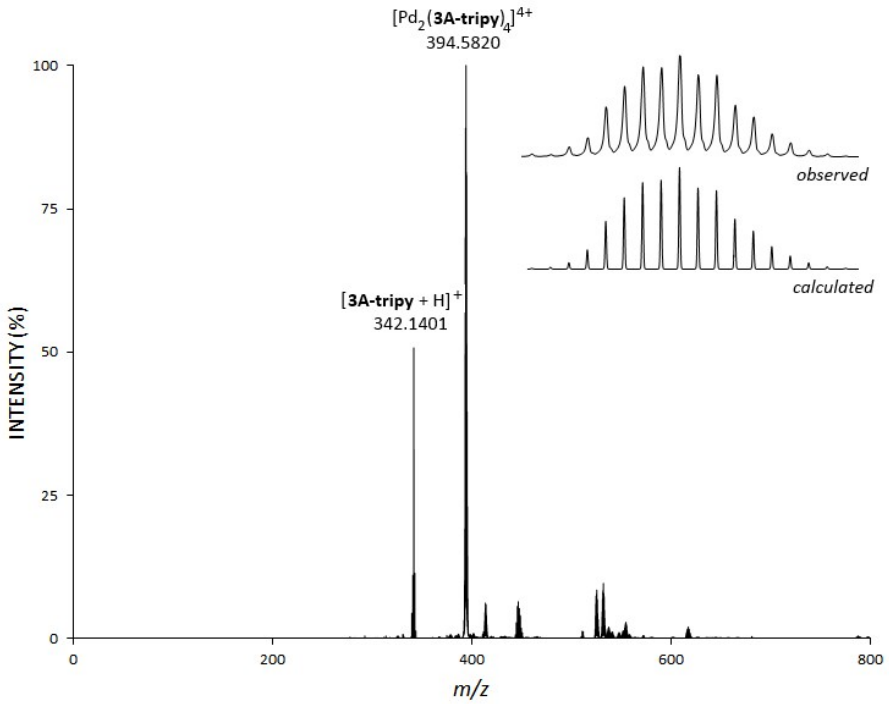

Figure S2.1 HR ES mass spectrum (DMSO/CH_3CN) of $[Pd_2(\mathbf{3A\text{-}tripy})_4](BF_4)_4$.

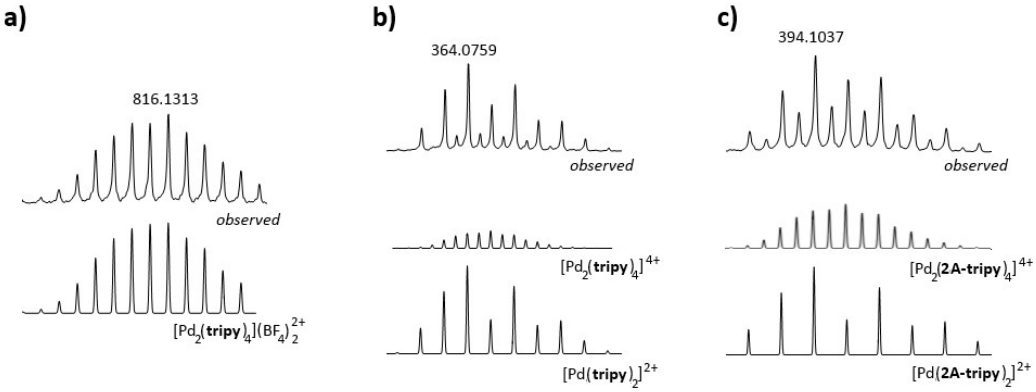

Figure S2.2 Partial HR ES mass spectra for **a)** $[Pd_2(\mathbf{tripy})_4](BF_4)_4$ (in CH_3CN), **b)** $[Pd_2(\mathbf{tripy})_4](NO_3)_4$ (in DMSO/CH_3CN) and **c)** $[Pd_2(\mathbf{2A\text{-}tripy})_4](BF_4)_4$ (in DMSO/CH_3CN), with observed spectra above and calculated middle and/or below.

3 Selected NMR spectral data

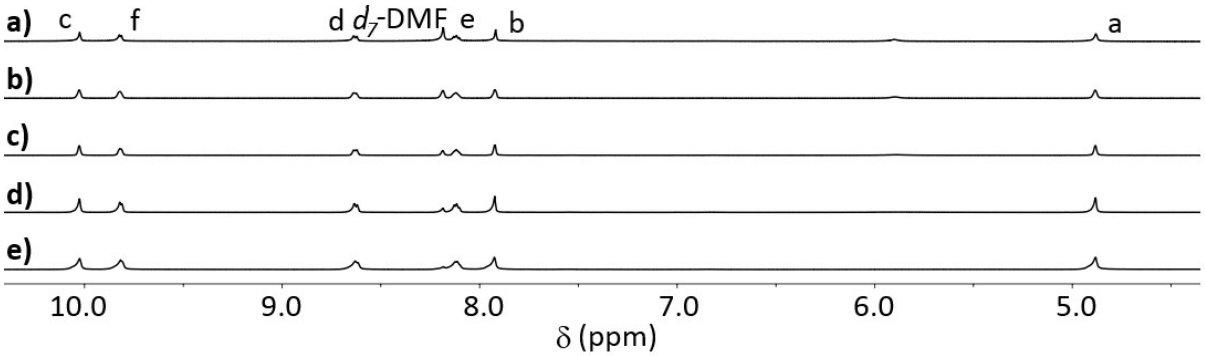

Figure S3.1 Partial ^{1}H NMR spectra (500 MHz, d_7-DMF , 298 K) of $[Pd_2(\mathbf{tripy})_4](BF_4)_4$ at a) 1.25 mM, b) 2.5 mM, c) 5 mM, d) 10 mM, e) 20 mM. ^{1}H DOSY NMR on these samples gave the same diffusion coefficients in all cases.

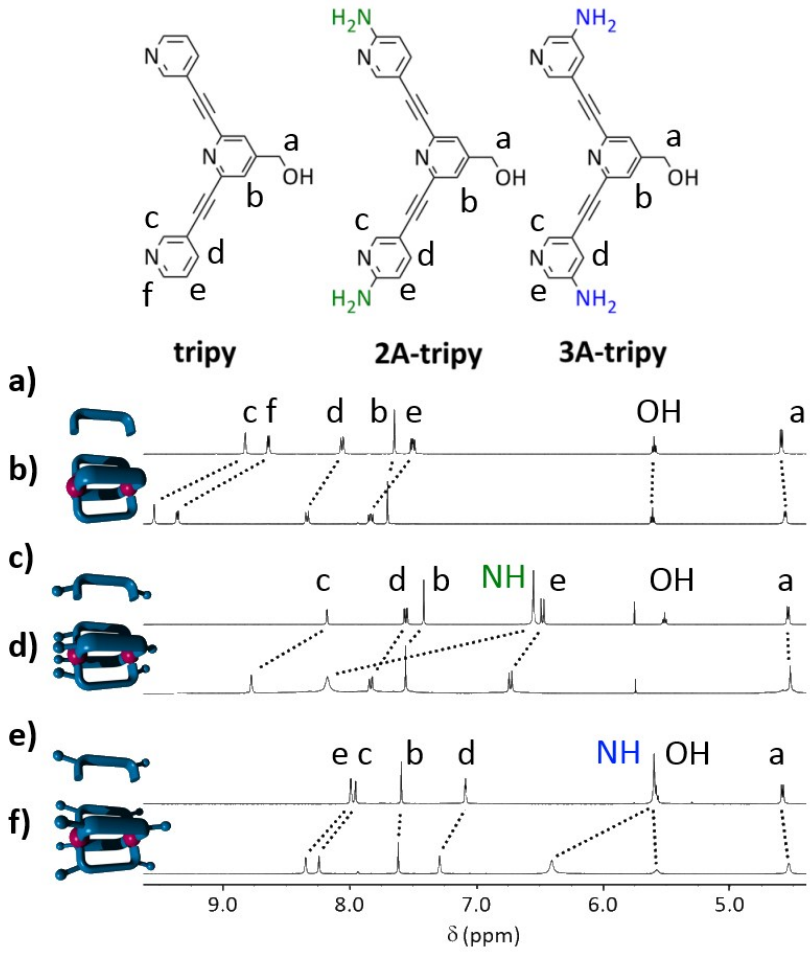

Figure S3.2 Partial ^{1}H NMR spectra (298K, 500 MHz, d_6-DMSO) of a) **tripy** and $[Pd_2(\mathbf{tripy})_4](BF_4)_4$, b) **2A-tripy** and $Pd_2(\mathbf{2A\text{-}tripy})_4](BF_4)_4$, and c) **3A-tripy** and $[Pd_2(\mathbf{3A\text{-}tripy})_4](BF_4)_4$.

Table S3.1 ^{1}H DOSY NMR–derived diffusion coefficients (*D*) for compounds (500 MHz, d_6-DMSO, 298 K).

Compound	Diffusion coefficient (*D*) x 10^{-10} m^2 s^{-1}	
	Ligand(s)	Cage
tripy	2.34	1.03
2A-tripy	1.73	0.89
3A-tripy	1.90	0.97

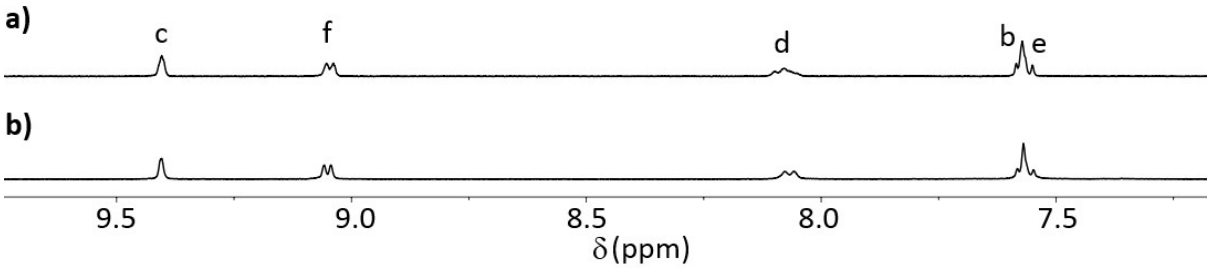

Figure S3.3 Partial ^{1}H NMR stacked spectra (400 MHz, D_2O, 298 K) of a) $[Pd_2(\mathbf{tripy})_4](NO_3)_4$ and b)) $[Pd_2(\mathbf{tripy})_4](NO_3)_4$ + 10 equivalents cisplatin.

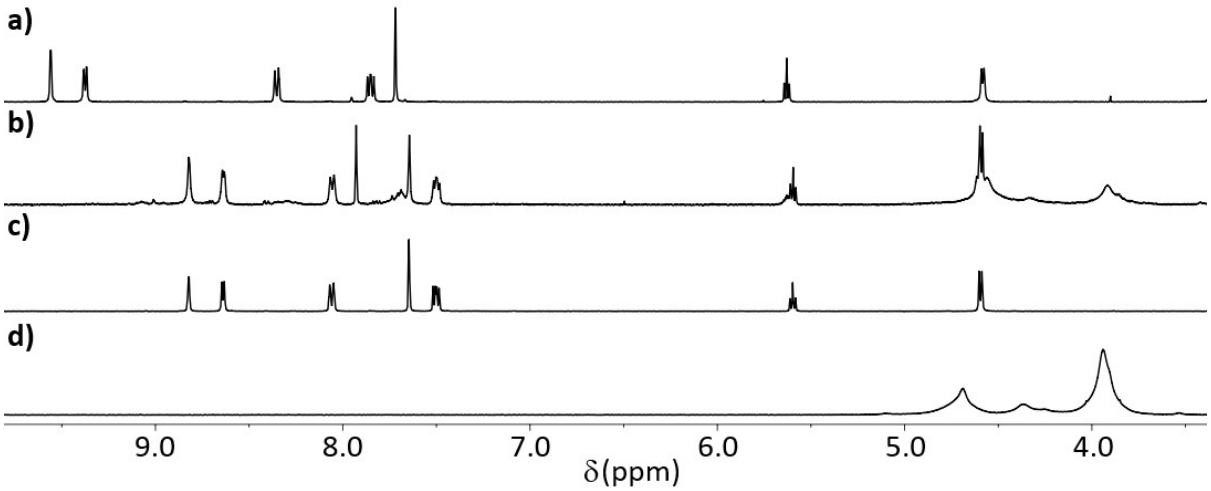

Figure S3.4 Partial ^{1}H NMR stacked spectra (400 MHz, d_6-DMSO, 298 K) of a) $[Pd_2(\mathbf{tripy})_4](BF_4)_4$ and b) $[Pd_2(\mathbf{tripy})_4](BF_4)_4$ + cisplatin, c) **tripy**, d) cisplatin.

4 Stability studies

All time course studies were carried out in a 3:2 d_6-DMSO/D_2O solvent mixture on a Varian 500 MHz AR spectrometer at 298 K. The concentration of the $[Pd_2L_4]^{4+}$ architectures was in all cases 3 mM. Testing was carried out against histidine, cysteine and tetramethylammonium chloride. Four equivalents of histidine and cysteine or eight equivalents of chloride were used. A reference sample of each dipalladium architecture at 3 mM concentration without nucleophile was used for time zero. The amount of complex still present over time in comparison to at time zero was calculated through comparison of the integration of the peak found at highest chemical shift (H_c) to the reference peak of trimethylsilyl propanoic acid, with additional comparison to the integration of peak belonging to the same proton in the free ligand.

4.1 Histidine

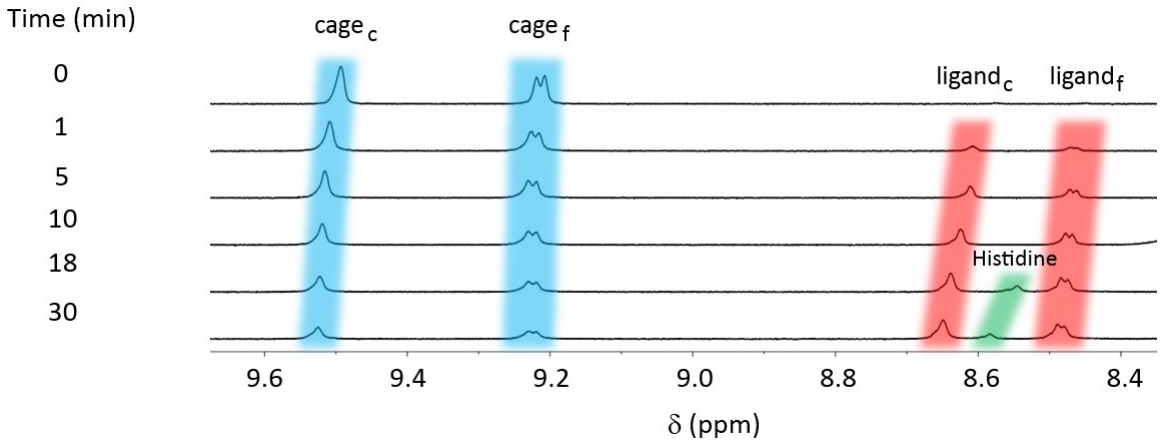

Figure S4.1 Time course partial ^{1}H NMR stacked plot of $[Pd_2(\mathbf{tripy})_4](BF_4)_4$ against 4 equivalents histidine (500 MHz, 3:2 d_6-DMSO/D_2O, 298 K). Colour coding: cage, free ligand, histidine.

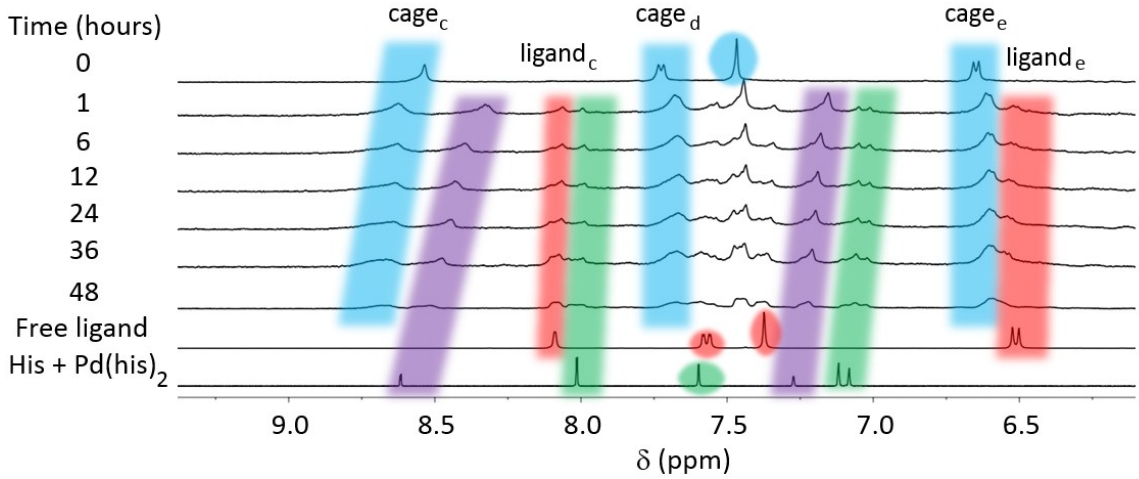

Figure S4.2 Time course partial ^{1}H NMR stacked plot of $[Pd_2(\mathbf{2A\text{-}tripy})_4](BF_4)_4$ against 4 equivalents histidine (500 MHz, 3:2 d_6-DMSO/D_2O, 298 K). Colour coding: cage, free ligand, free histidine, bis(histidine)palladium(II) complex.

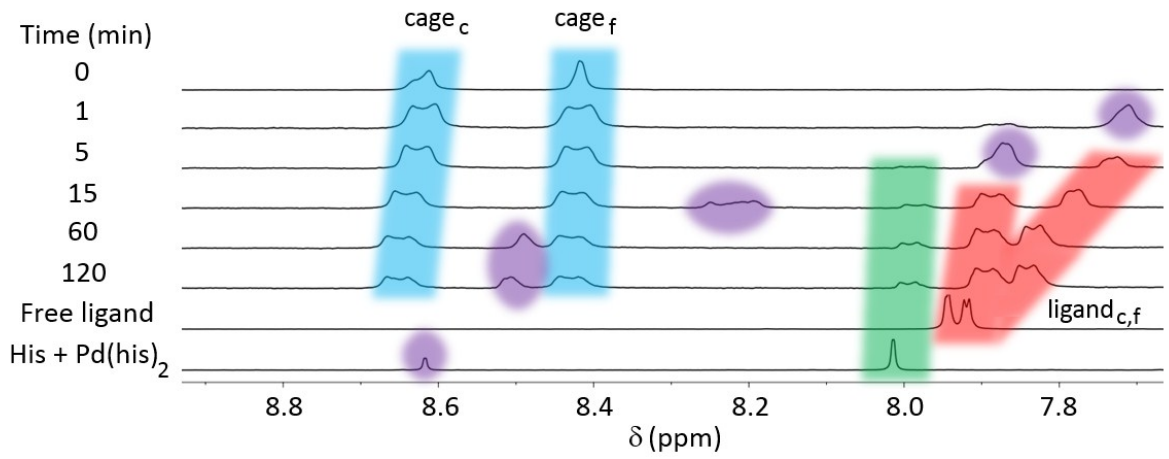

Figure S4.3 Time course partial ^{1}H-NMR stacked plot of $[Pd_2(\mathbf{3A\text{-}tripy})_4](BF_4)_4$ against 4 equivalents histidine (500 MHz, 3:2 d_6-DMSO/D_2O, 298 K). Colour coding: cage, free ligand, free histidine, bis(histidine)palladium(II) complex.

4.2 Cysteine

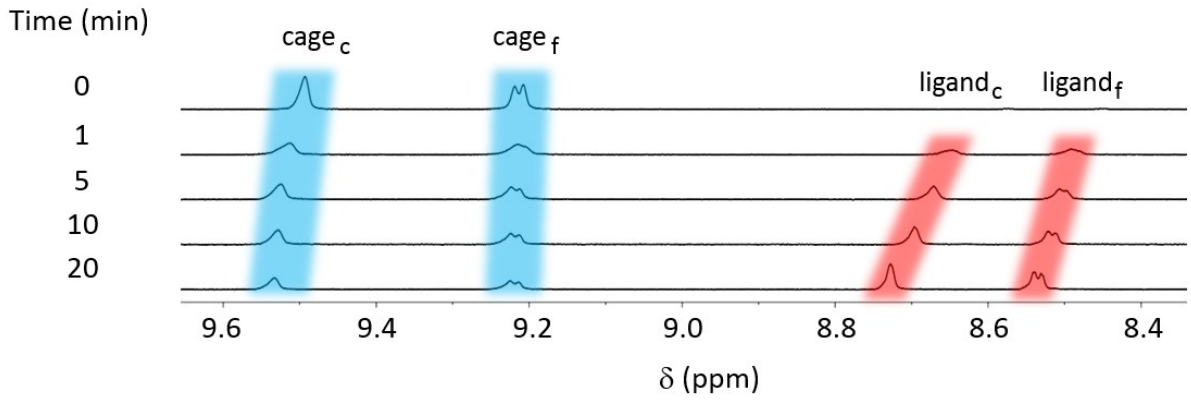

Figure S4.4 Time course partial ^{1}H-NMR stacked plot of $[Pd_2(\mathbf{tripy})_4](BF_4)_4$ against 4 equivalents cysteine (500 MHz, 3:2 d_6-DMSO/D_2O, 298 K). Colour coding: cage, free ligand.

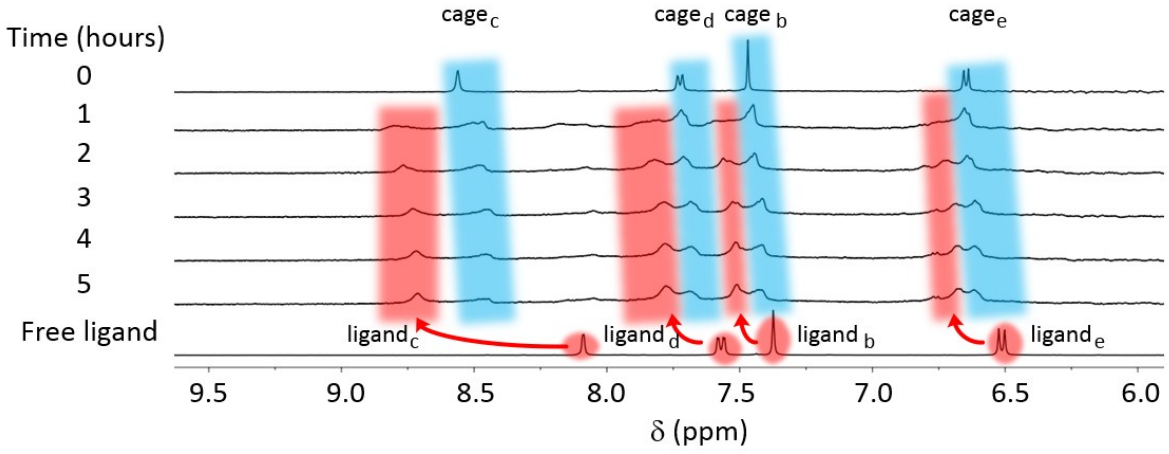

Figure S4.5 Time course partial ^{1}H-NMR stacked plot of $[Pd_2(\mathbf{2A\text{-}tripy})_4](BF_4)_4$ against 4 equivalents cysteine (500 MHz, 3:2 d_6-DMSO/D_2O, 298 K). Colour coding: cage, free ligand.

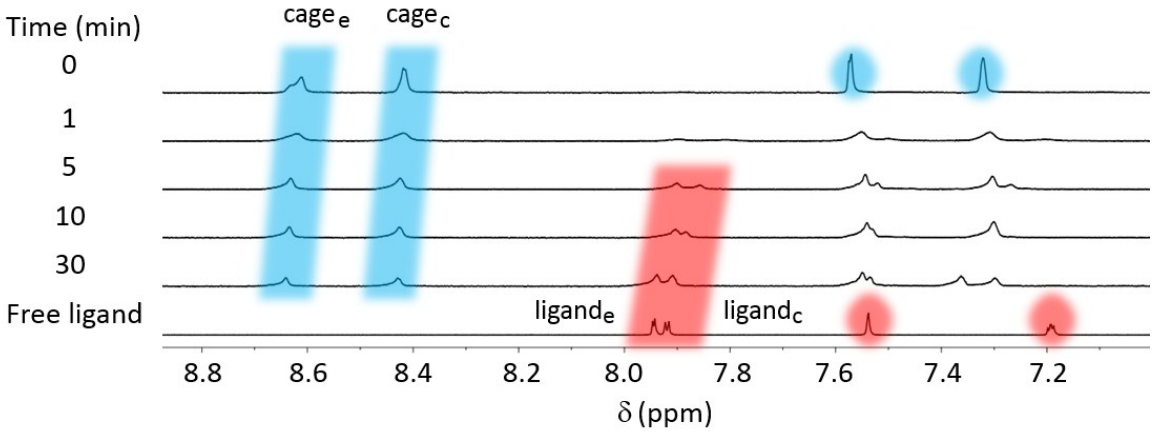

Figure S4.6 Time course partial ^{1}H-NMR stacked plot of $[Pd_2(\mathbf{3A\text{-}tripy})_4](BF_4)_4$ against 4 equivalents cysteine (500 MHz, 3:2 d_6-DMSO/D_2O, 298 K). Colour coding: cage, free ligand.

4.3 Chloride

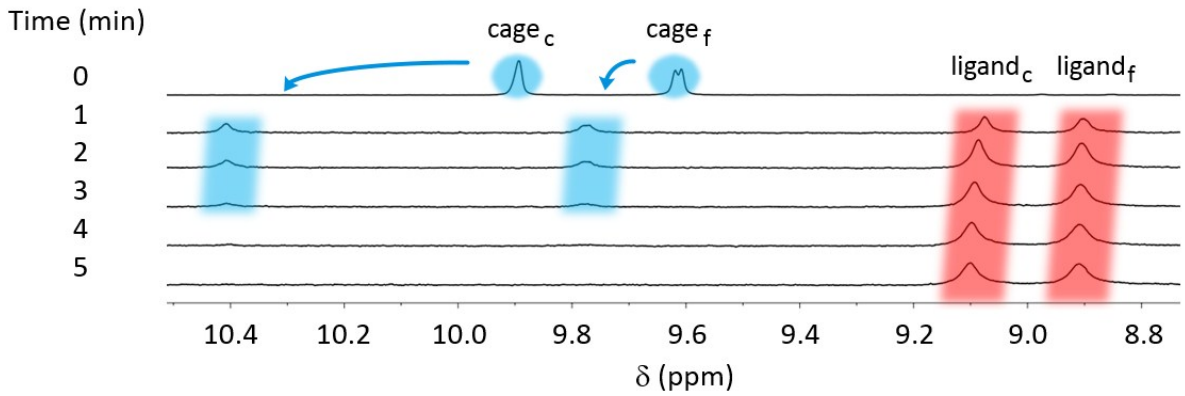

Figure S4.7 Time course partial ^{1}H-NMR stacked plot of $[Pd_2(\mathbf{tripy})_4](BF_4)_4$ against 8 equivalents tetramethylammonium chloride (500 MHz, 3:2 d_6-DMSO/D_2O, 298 K). Colour coding: cage, free ligand.

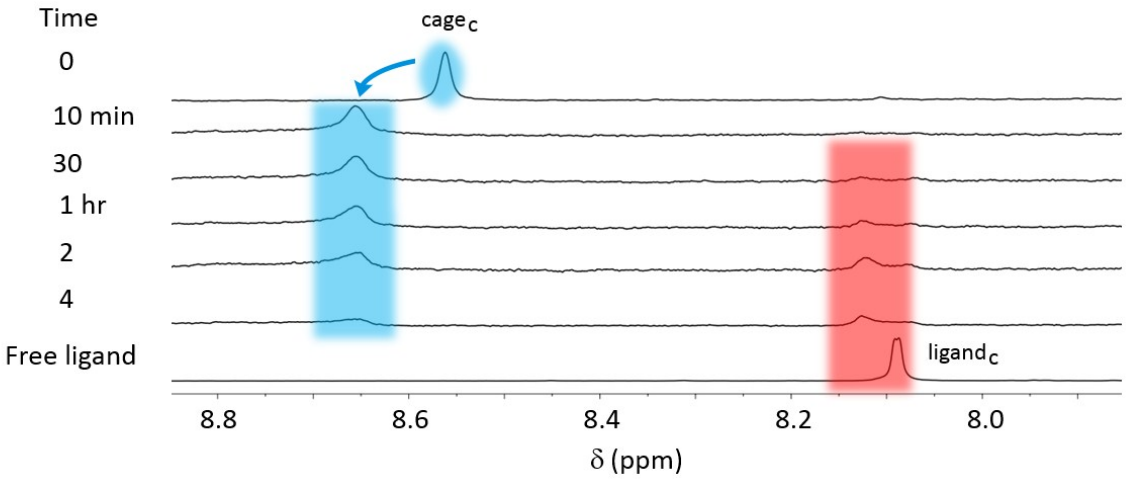

Figure S4.8 Time course partial ^{1}H-NMR stacked plot of $[Pd_2(\mathbf{2A\text{-}tripy})_4](BF_4)_4$ against 8 equivalents tetramethylammonium chloride (500 MHz, 3:2 d_6-DMSO/D_2O, 298 K). Colour coding: cage, free ligand.

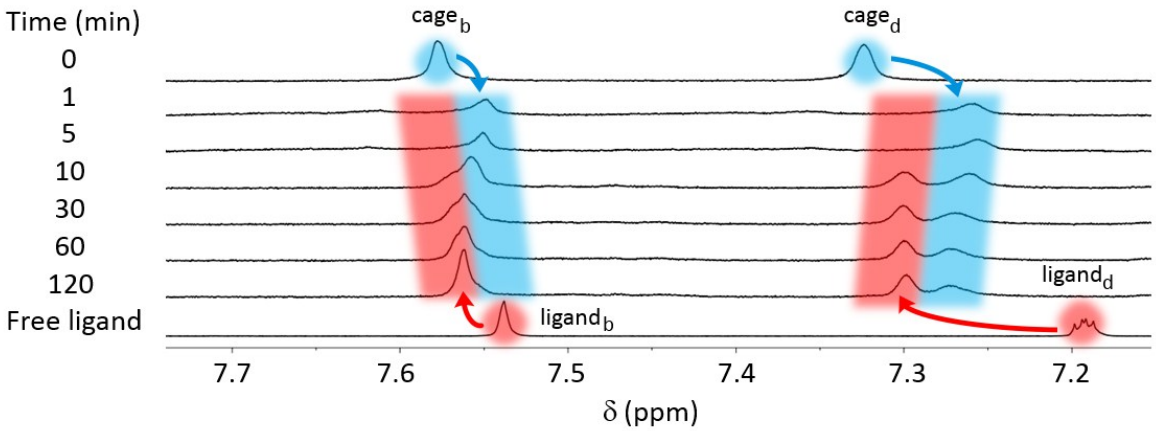

Figure S4.9 Time course partial ^{1}H-NMR stacked plot of $[Pd_2(\mathbf{3A\text{-}tripy})_4](BF_4)_4$ against 8 equivalents tetramethylammonium chloride (500 MHz, 3:2 d_6-DMSO/D_2O, 298 K). Colour coding: cage, free ligand.

5 X-ray Data

5.1 $[Pd_2(tripy\text{-}2A)_4](BF_4)_4$

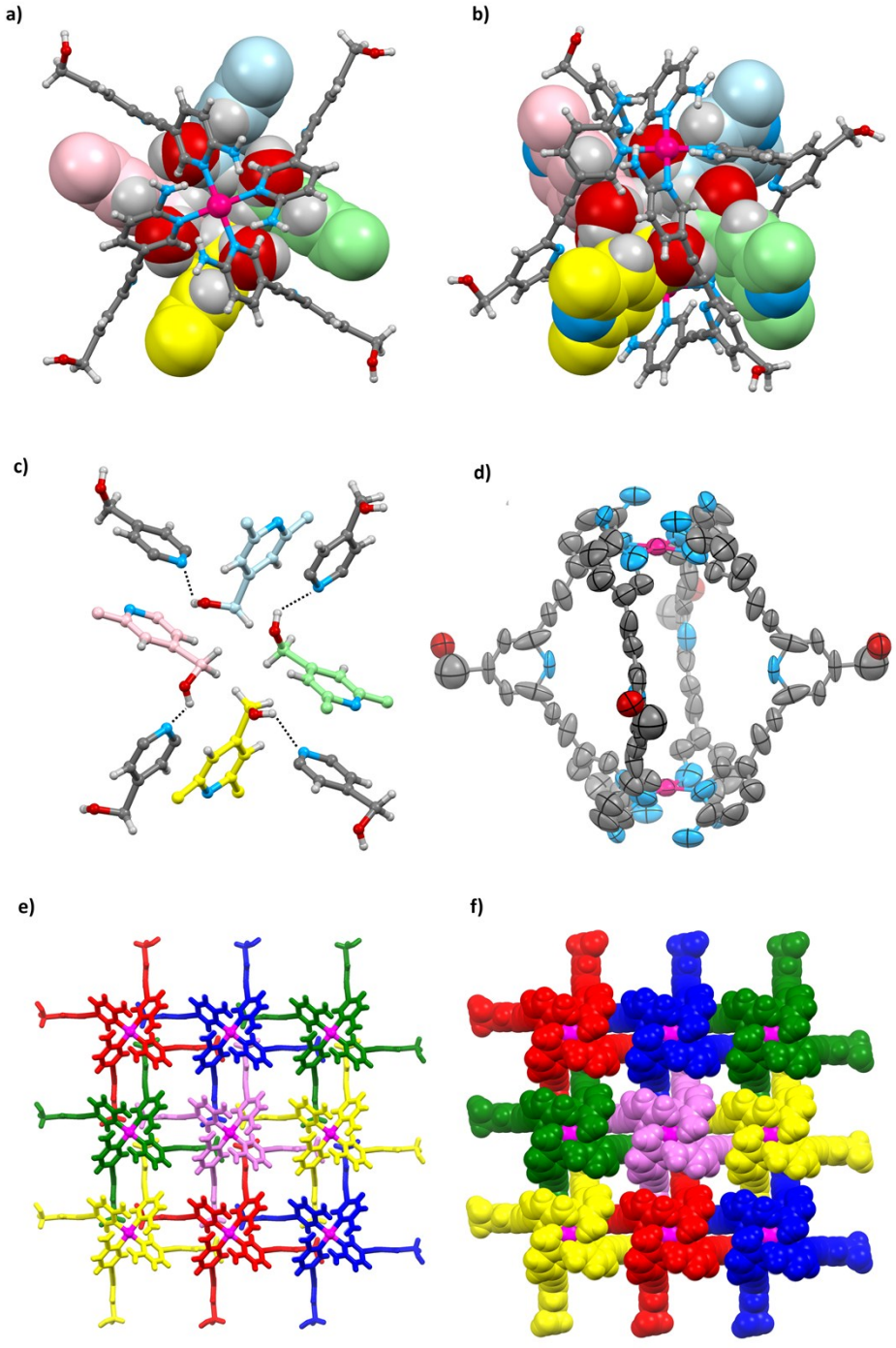

Figure S5.1 Ball and stick representation of $[Pd_2(\mathbf{2A\text{-}tripy})_4](BF_4)_4$ showing the filling of the cavity by the methylene alcohol substituents (shown in spacefilling view in yellow, green, blue and pink) from the four neighbouring cages in the lattice, shown from a) above and b) a more tilted view. The proposed hydrogen bonding network within the cavity is shown in c) Only the central pyridyl ring, the adjacent alkyne carbon, and the methylene alcohol are shown of the interpenetrating cages. An ellipsoid plot (no hydrogen atoms or counterions, ellipsoids 50% probability) in d). The extended interpenetrating network is shown in e) (tube view) and f) (spacefilling view). Due to poor data, hydrogen bonding distances are not included.

Platon squeeze void number	Platon squeeze void average x	Platon squeeze void average y	Platon squeeze void average z	Platon squeeze void volume	Platon squeeze void count electrons	Platon squeeze details
1	0.000	0.000	0.077	18	10	H_2O
2	0.000	0.500	0.253	127	43	BF_4
3	0.000	0.000	0.500	246	110	$2 \times BF_4$ CH_3CN
4	0.000	0.500	0.747	127	43	BF_4
5	0.000	0.000	0.923	18	10	H_2O
6	0.500	0.000	0.253	127	43	BF_4
7	0.500	0.000	0.747	127	43	BF_4
8	0.500	0.500	0.000	249	136	$2 \times BF_4$ $2 \times CH_3CN$ H_2O
9	0.500	0.500	0.432	23	11	H_2O
10	0.500	0.500	0.568	23	11	H_2O

5.2 Cavity comparison of $[Pd_2(2A\text{-}tripy)]^{4+}$ and $[Pd_2(tripy)_4]^{4+}$

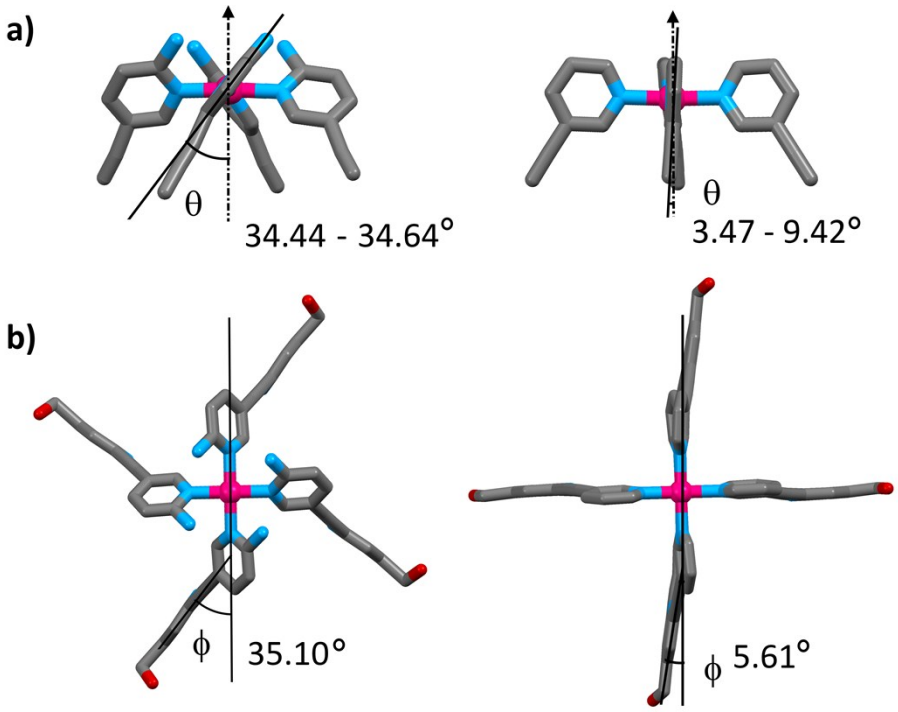

Figure 5.2 Tube depictions of the crystal structures of $[Pd_2(\mathbf{2A\text{-}tripy})_4]^{4+}$ and $[Pd_2(\mathbf{tripy})_4]^{4+}$[1] showing a) swivelling of the coordinating pyridine rings relative to the principal rotation axis (θ), and b) twisting of the central pyridine ring out of the coordination plane (ϕ). Colours: carbon grey, nitrogen blue, oxygen red, palladium magenta. Counterions and/or hydrogen atoms and solvent molecules omitted for clarity.

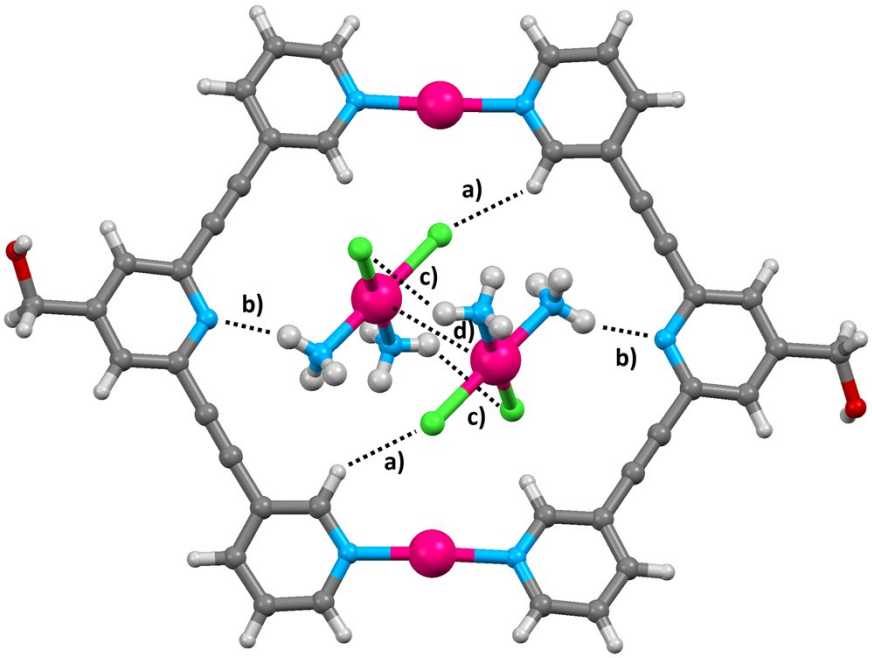

Figure 5.3 Ball and stick representation showing partial $[Pd_2(\mathbf{tripy})_4]^{4+}$ cage crystal structure with two cisplatin molecules encapsulated,[1] with interactions as dotted lines. Interactions: a) chloride----hydrogen, b) amino-----pyridine, c) inter-cisplatin amino----chloride, and d) inter-cisplatin platinum(II)-----platinum(II). Colours: carbon grey, nitrogen blue, oxygen red, palladium magenta. Note that these binding interactions have previously been seen in solid state structures of analogous systems.[2]

5.3 Crystallographic data

Identification code		$[Pd_2(2A\text{-}tripy)_4](BF_4)_4$ /dp549 CIF #: 1439952
Empirical formula		$C_{80}H_{52}N_{16}O_4Pd_2$ $(C_{80}H_{60}B_4F_{16}N_{20}O_4Pd_2 \cdot C_3H_{9.5}N_{1.5}O_{2.5})^a$
Formula weight		1514.8 (2032.14)[a]
Temperature		100(1) K
Wavelength		1.54184 Å
Crystal system		Tetragonal
Space group		*P4/m*
Unit cell dimensions	$\alpha = 11.3213(11)$ Å	$\alpha = 90°$
	b = 11.3213(11) Å	$\beta = 90°$
	c = 34.953(4) Å	$\gamma = 90°$
Volume		4480.0(10) $Å^3$
Z		2
Density (calculated)		1.122 Mg/m^3 (1.506)[a]
Absorption coefficient		3.643 mm^{-1} (4.095)[a]
F(000)		1536 (2052)[a]
Crystal size		0.2028 x 0.1121 x 0.0485 mm^3
Theta range for data collection		3.794 to 73.702°
Index ranges		-13<=h<=14, -13<=k<=12, -39<=l<=43
Reflections collected		34358
Independent reflections		4572 [$R_{(int)}$ = 0.1650]
Completeness		100.0% to theta = 67.684°
Absorption correction		Gaussian
Max. and min. transmission		1.00000 and 0.56661
Refinement method		Full-matrix least-squares on F^2
Data / restraints / parameters		4572 / 97 / 237
Goodness-of-fit on F2		1.179
Final R indices [I>2sigma(I)]		R_1 = 0.1445, wR_2 = 0.4487
R indices (all data)		R_1 = 0.2249, wR_2 = 0.4447
Largest diff. peak and hole		0.776 and -0.678 $e.Å^{-3}$
Absolute structure parameter		-

[a] alternative parameters, derived from empirical formula including SQUEEZED solvent.

6 References

[1] A. Schmidt, V. Molano, M. Hollering, A. Poethig, A. Casini, F. E. Kuehn, *Chem. - Eur. J.* **2016**, *22*, 2253-2256.

[2] aJ. E. M. Lewis, A. B. S. Elliott, C. J. McAdam, K. C. Gordon, J. D. Crowley, *Chem. Sci.* **2014**, *5*, 1833-1843; bJ. E. M. Lewis, C. J. McAdam, M. G. Gardiner, J. D. Crowley, *Chem. Commun.* **2013**, *49*, 3398-3400.